Genetic Regulation of Retinal Cells by Variation of Underlying Elastic Modulus

---

A Dissertation presented to

the faculty of the Department of Physics

University of Houston

In Partial Fulfillment

of the Requirements of the Degree

Doctor of Philosophy

By

Joshua Tyler Davis

May 2013

Genetic Regulation of Retinal Cells by Variation of Underlying Elastic Modulus

_____

Joshua Tyler Davis

APPROVED:

_____

Dr. William Foster, Chair

_____

Dr. Lawrence Pinsky

_____

Dr. John Miller

_____

Dr. Deborah Otteson

_____

Dean, College of Natural Science and Mathematics

Genetic Regulation of Retinal Cells by Variation of Underlying Elastic Modulus

---

An Abstract of a Dissertation

Presented to

the Faculty of the Department of Physics

University of Houston

In Partial Fulfillment

of the Requirements for the Degree

Doctor of Philosophy

By

Joshua Tyler Davis

May 2013

ABSTRACT

A major breakthrough in the development of engineering hydrogels for regenerative medicine occurred when it was noticed that when cells are plated on substrates of different stiffnesses undergo certain conformational changes in their cytoskeleton. Specifically, the tension in cytoskeleton of the cells on the substrates increased with stiffness. Many different cell types were noted to have a larger spread area and the presence of stress fibers. This was called, by Donald Ingber and Buckminster Fuller, tensegrity and is likened to a tent erected in different soils. The tent poles act as the skeleton with the outer covering as the membrane, the poles create tension on the pegs and, if they are not planted in firm ground, the tent snaps back. It has also been shown that pluripotent cells will develop into different specialized cells purely under the influence of substrate stiffness. This finding implies an alteration of the genetic regulation arising from the tension in the cytoskeleton. Hence, a structure that does not exist inside the nucleus is changing the transcription of DNA. How this non-chemical signaling occurs, as well as which genes are affected in which cells and what stiffness levels trigger these changes, is now

what needs to be investigated. We began working with a retinal cell line to see if these unique cells change genetic expression in the same way, which might help to explain the buildup of scar tissue in the retina after reattachment surgery. This scar tissue (proliferative vitreoretiopathy), in many cases, leads to secondary retinal detachments. We discovered that there were many changes, both physically and genetically, that Müller cells undergo when exposed to varying levels of substrate stiffness. Changes found include varying expression of different extracellular matrix genes, an inverse relationship between the amount of phagocytosis and substrate stiffness, and determining that not only is protein expression of the cells different across substrates, the time of peak expression varies.

Contents

INTRODUCTION

Disease Relevance

In rhematogenous retinal detachment a hole in the retina is created, and due to the shear forces applied to the retina by the vitreous humor, the retina pulls away from the underlying retinal pigment epithelial (RPE) layer of cells. This sub-retinal space is then filled with vitreous fluid. To be repaired, the vitreous filling the eyeball must be removed surgically. Once it is removed, the retina can be attached manually and the tear sealed by coagulating the surrounding tissue with a laser. The problems arising from replacing the excised vitreous shall be covered in a different section.

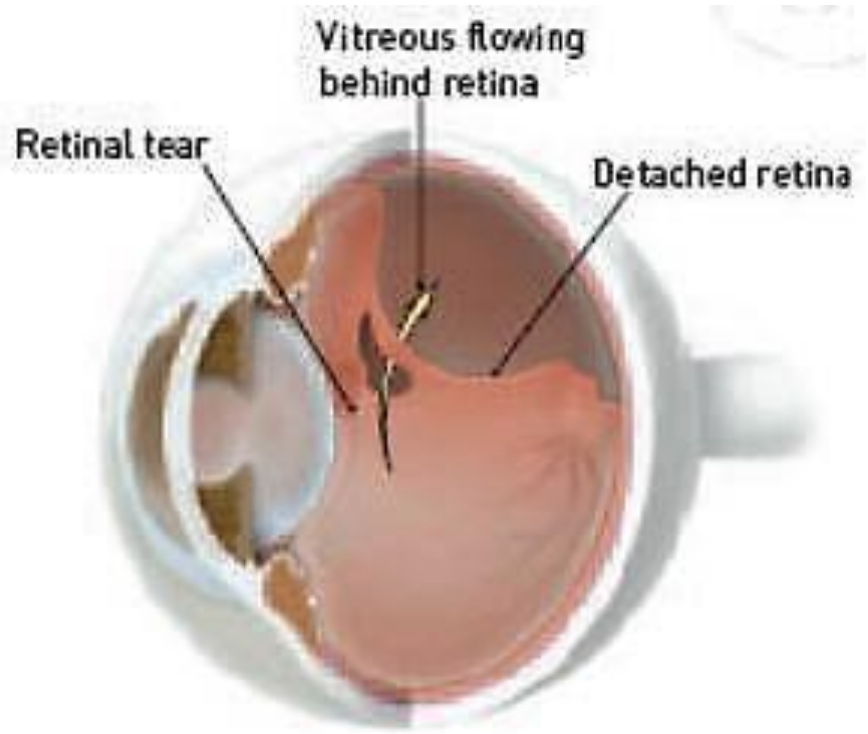

Figure I.1: Image of retinal detachment (Carolina Retina Institue carolinaretinadoc.com)

It has been noted on many occasions that repairing a retinal detachment will lead to the presence of gliosis in the retinal layers[1]. The gliosis can proliferate, causing the growth of fibrotic tissue. This fibrotic tissue can then contract, which leads to secondary detachment[2]. This condition is called proliferative vitreoretinopathy (PVR).

Glia/Gliosis

Glial cells are present throughout the nervous system. They provide a structural framework for neurons and also, provide nutrient transport[3]. In addition to the structural framework, glial cells also insulate neurons from each other, by means of the myelin sheath[4], and are responsible for the removal of dead neurons[5]. In the human brain there is a glial cell for every neuron[6].

Gliosis, or Glial scar formation, is the process by which the body attempts to repair damage to neuronal tissue. After damage occurs, numerous cell types remove the dead tissue. Glial cells then begin to proliferate rapidly to fill the empty space that has been created. The purpose of this is to maintain the structural integrity of the tissue and

has the effect of preventing not only microbial contamination, but also neovascularization from penetrating[7].

Gliosis does have a detrimental effect as well. The pseudopodia and stress fibers created in an effort to fill the void in the neural tissue actually act as a physical barrier to the growth of axons[7]. The formation of the Glial scar is necessary, as inhibition of it has been shown to cause impairments to the blood brain barrier[8]. These stress fibers change the local environment by increasing the surrounding stiffness of nearby cells. This causes a problem as we will show that a cell's stiffness increases linearly with that of its environment so that local cell stiffness will increase. As this stiffness migrates away from the scar, so too can the scar. This is seen in rhematogenous retinal detachment.

Müller Glia

Müller glia play an important role in the retina, not just as structural components but also in repair and development. The cells facilitate the degradation of neurotransmitters such as acetylcholine and gamma-aminoburytic acid[9]. The degradation of these

neurotransmitters helps neuronal function and maintains a beneficial microenvironment for the retina. The cells also induce glutamine synthetase activity[10], an enzyme which converts the neurotransmitter glutamate and cytotoxic ammonia into glutamine[11, 12]. They are not only a site of enzymatic activity, it has also been suggested that Müller cells are primarily responsible for the penetration and funneling of light through the retina and to the photoreceptors[13].

In embryonic development, Müller glia have been shown to have an important role in both growth and differentiation of retinal cells[14]. As Müller cells span the entire retina, their positioning in development of the embryonic retina seems to act as a guide for differentiation of retinal layers, particularly the axons and synapses of neurons[15, 16].

It has been shown that, in fish, the growth of new neuronal cells does not stop with maturity[17]. Instead, the number of neurons grows if the size of the retina grows. The cells will also proliferate to fill in any voids formed by all potential forms of trauma[18]. Following injury, Müller glia have been shown to migrate into the area of damaged or

removed tissue and proliferate similar to Schwann cells[19]. It has also been shown in zebrafish that the inhibition of proliferation in Müller glia blocks the ability to repair damaged retina[20]. As the cells are repairing the trauma, the Müller cells are believed to have the ability to dedifferentiate to a retinal progenitor cell[21]. These multipotent progenitors can then redifferentiate to replace any cells that were unalterably injured specifically in fish species. It should be noted that the results found with retinal repair, and the influence of Müller cells on this repair, has not been seen in mammals and work is being done to find out what is creating the difference between mammalian and fish species so that this repair can progress. In summary, Müller cells are interesting not only as a model glial cell, but because they seem to behave in a number of ways that are critical for retinal regeneration, including turning into retinal precursor (or ‘stem’) cells.

Substrates

In cell culture, polymer substrates can be used to alter the local environment of cells either structurally, chemically, or mechanically. The polymer substrates are created using a mixture of specific

amounts of different inorganic or organic molecules, including proteins. Within this mixture, the molecules react and begin attaching to each other in a crosswise pattern, much like a haphazard cubic lattice. As the concentration of molecules in the mixture is raised, more connections can be made, which decreases the pore size. This, in turn, stiffens the structure. To ensure the stiffness is appropriate for the cells involved, the different concentrations must be measured, both by atomic force microscopy and rheology. Atomic force microscopy (AFM) uses a force on a cantilever of known size to deform the gel and measure its elastic modulus. Rheometers measure the shear stress of a substance either linearly or rotationally to get the bulk modulus of the system.

After stiffness is determined, cell function can be studied. In three-dimensional substrates, such as polyethylene glycol and collagen gels, the gels are polymerized with the cells already in the mixture so that, when the lattice is formed, the cells will occupy the voids. This gives the benefit of allowing the cells to attach themselves in a more natural, three-dimensional environment as well as providing physiological barriers to growth and locomotion. One problem is that

two or more different proteins are used to create the crosslinked gel. This means that you cannot independently control the density of proteins the cells attach to or the stiffness of the gel. Also, these proteins will not be the same as the normal extracellular matrix in tissue. Because the matrix proteins are part of the structure of the gel, cells will be more sensitive to the local changes in stiffness that naturally occur due to variations in pore size. As the extracellular matrix, both basement membrane and interstitial matrix, is a polymer, increasing the number of attachment points will increase the ability to crosslink and thus the stiffness. Recently it has been shown that the number of binding sites between collagen fibrils may be just as important as the stiffness of the underlying substrate[22].

The gels themselves are also highly variable in composition and, as such, not currently ideal for attempting to understand the cellular response[23]. The chemical environment of the cell can also be altered by diffusing growth factors or other compounds, which can then be modulated by the controlled expansion or contraction of the gel due to different physical cues, such as temperature or pH[24]. This method is now being studied as a directed drug delivery system.

Two-dimensional gels have become standard for studying the effect of stiffness on cells, both for their ease of use and the ability to independently control the chemical and mechanical environment. This is why we have been chosen for all the protocols used in this thesis.

Atomic Force Microscopy

The atomic force microscope was created by Binning, Quate, and Gerber in 1986 for use in scanning the topography of a surface with a resolution below the diffraction limit. It is also useful in measuring forces on a small scale, down to the intermolecular forces. It uses a very fine tipped cantilever to scan the surface of a substrate and the position of this cantilever is measured by laser or electron beam, so that even nanometer deflections can be interpreted. The material properties can also be read. With a force applied to the cantilever, the beam can measure the total displacement. The force applied to a known cantilever curvature will give a stress, and the displacement of the cantilever into the substrate will result in a strain.

$$E = \frac{stress}{strain} = \frac{F/A}{\Delta L/L}$$

When combining these you can find the elastic modulus, and since it is a localized stress that is being applied the result is the elastic modulus of the surface and not the bulk modulus. The bulk modulus can be found by placing the entire substrate under the same stress and measuring the deformation.

Problems arise when working with the atomic force microscope on soft polymers[25], the cantilever tip has a radius of curvature on the order of tens of nanometers which is small enough to pierce soft films. To alleviate this, microspheres are attached to the tip to give a larger radius of curvature and therefore decrease the stress for the force applied. The other problem that was encountered was that the theoretical model used to solve for the Young's modulus, the Hertz model:

$$F = \frac{2}{\pi}\frac{E}{1-\nu^2}\delta^2\tan(\alpha)$$

Which assumes an infinite thickness of the polymer. Since we are not dealing with an infinite thickness and the polymer is bound to a surface that is much more rigid, a correction needs to be made to account for the fact that the atomic force microscope is actually

detecting the combined modulus of the gel and its underlying boundary. This correction was done by Dimitriadis et al.[25], by using a method of images.

$$F = \frac{4E}{3(1-\nu^2)} R^{1/2}\delta^{3/2}\left[1 - \frac{2\alpha_o}{\pi}\chi + \frac{4\alpha_o^2}{\pi^2}\chi^2 - \frac{8}{\pi^3}\left(\alpha_o^3 + \frac{4\pi^2}{15}\beta_o\right)\chi^3 + \frac{16\alpha_o}{\pi^4}\left(\alpha_o^3 + \frac{3\pi^2\beta_o}{5}\right)\chi^4\right]$$

where $\chi = \frac{\sqrt{R\delta}}{h}$

In this equation, α_o and β_o are functions of the Poisson ratio v which varies depending on whether the polymer is bound to the underlying substrate or if it is allowed to slip. With these corrections applied, correlations between the measurements by atomic force microscopy and macroscopic measurements are attainable. Not only this, but as the substance is thickened the mapping by Hertzian Theory approaches and eventually coincides with the constant measurements given with the thickness correction.

Extracellular Matrix

As stated previously, the idea of extracellular cues influencing the function of cells has been studied by investigators. Not only have researchers looked at the cytoskeletal structure and organization, but also motility, speed, and traction forces applied at the focal adhesions. It has been debated what in the environment the cells are responding to, whether it is the chemical composition or the underlying substrate. What is known is that the extracellular matrix (ECM) is responsible for support of cells, the alleviation and application of stresses to cells, the regulation of communication between cells, and the binding of growth factors and other chemical signals[26]. The matrix is also essential in wound healing and fibrosis. Components of the extracellular matrix are produced by cells and secreted by exocytosis to form a polymer with pre-existing matrix components[27].

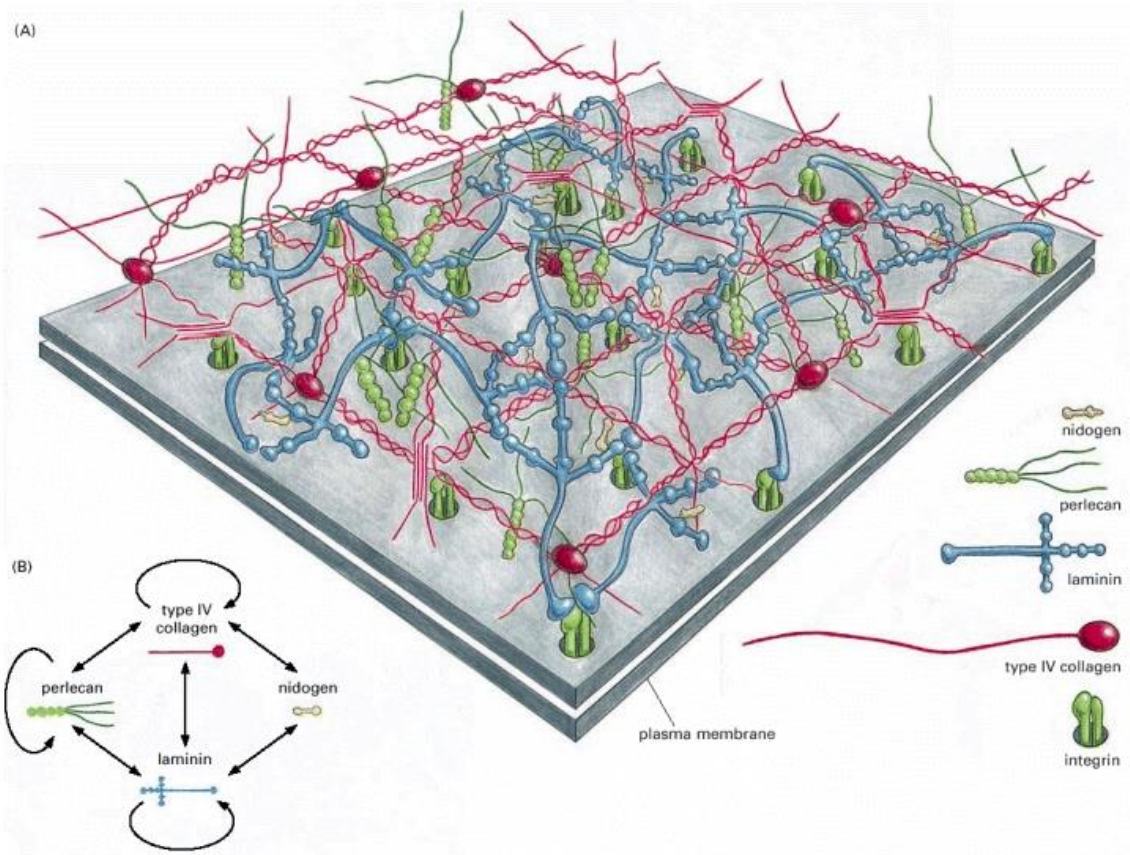

Figure I.2: Structure of the basal lamina (Molecular Biology of the cell Alberts, et al.[28])

Cells interact with this extracellular matrix polymer by means of cell surface proteins called integrins. Whether it is by focal adhesions, connecting the extracellular matrix to the actin cytoskeleton, or by hemidesmosomes, connecting the extracellular matrix to intermediate filaments, integrins will only bind specifically to either Laminin, Fibronectin, or other integrins[27]. Through integrins, the cells are able to sense the stiffness of the environment. As one would expect given the desire for objects in suspension to retain a spherical shape in order to minimize the energy of the system, the focal adhesions near the edges of cells (in the pseudopodia and stress fibers) are under a significantly higher tension than those near the nucleus[29, 30]. The higher tensions are only able to be supported when the stiffness of the underlying substrate is increased. When cells are plated on a gel of varying stiffness, the side of the cell in the direction of increasing stiffness is able to extend its stress fibers further thus increasing tension in that direction. From this idea was born durotaxis, or the ability of a cell to pull itself according to a change in mechanical properties.

My research has focused upon replicating environments which mirror the natural state of the cells, varying parameters in order to understand how changes in stiffness influence cellular behavior. In tissue engineering and regenerative medicine, it is important for the local environment to be as biomimetic as possible to both better understand how cells react to change and to learn how to keep detrimental changes from occurring in the body.

Procedures

Cell differentiation and level of gliotic activity were studied in several ways. First, we used qualitative real-time polymerase chain reaction (qPCR), which replicates strands of DNA specific to certain genes using DNA primers (Figure 3). Fluorescence is measured after each cycle of replication. As DNA is copied, double-stranded DNA is formed. A dye is present in each well which only fluoresces when constrained within double-stranded DNA. Therefore, since each cycle doubles the number of DNA strands (until the transcription factor or dye becomes the limiting reagent), the signal doubles at each pass. It

is only the starting amount of the gene that determines when the exponential growth occurs.

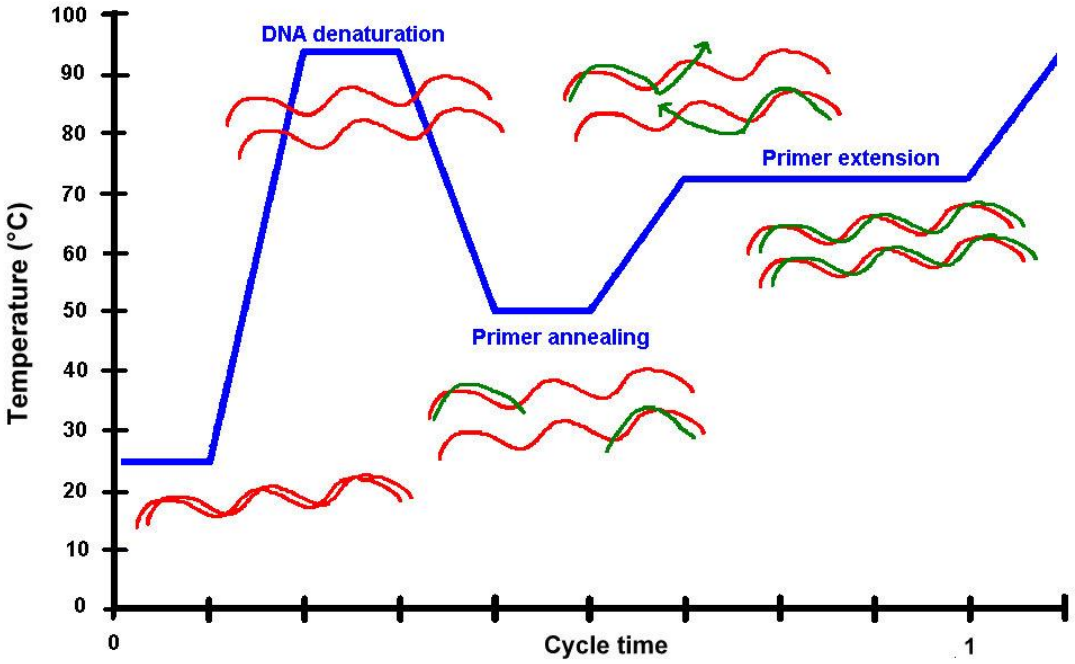

Figure I.3: Polymerase chain reaction as the DNA cycles

(http://www.mun.ca/biology/scarr/PCR_simplified.html)

The problem with this approach is that RNA transcription and protein translation do not always have a 1:1 correspondence. That is to say an increase in mRNA does not always mean an increase in protein. To find actual protein expression (a Western blot), the cells are lysed and the protein separated by centrifugation. These extracted proteins are chemically unwound and passed through a polyacrylamide gel by means of an electric current. When a high enough current is passed through the gel, the polar side chains in some amino acids are pulled toward the bottom of the gel. Because the proteins have varying lengths, they begin to be separated as the mean free path is much longer for the shorter strands. Once the proteins are properly separated, they can be transferred to a Nitrocellulose filter, again carried out by electric current. This Nitrocellulose filter is then placed in antibodies against a specific protein and tagged so chemiluminescence levels (in this case it is the breakdown of hydrogen peroxide into oxygen, causing a chemical reaction to emit light) and thus quantity of protein can be measured.

As a Western blot uses the protein of lysed cells, that is proteins that are within the cell at the time of cell lysis, it can be difficult to use this

method to analyze extracellular proteins. For that, an enzyme-linked immunosorbent assay (ELISA) is useful. In this technique, removing the cell media and testing it to see how much protein had built up in the media in the three days it had been in contact with the cells. A primary antibody is attached to the bottom of each well in the enyme-linked immunosorbant assay plate so that when the cell supernatant is added, the protein of interest will remain in the well. An identical antibody to that which is holding the protein to the bottom of the well is added to the well so that a type of protein “sandwich” is made. After the tagged secondary antibody is added, a reactive liquid is placed on top. The tag on the secondary antibody is an enzyme which causes a conversion in the solution resulting in a change in color, the degree of which depends upon the amount of secondary antibody present. The depth of color can be measured according to the absorbance of a certain wavelength (in this case 450nm) inside a spectrophotometer and comparing that value to the known standard.

Applications

Currently the repair of retinal detachment relies on either a gas bubble or silicon oil[31]. Because of this, there is a very unpleasant

recovery from the surgery, in which long periods of time must be spent face down or on one side. If instead a hydrogel of the right physical properties is used, not only could scar tissue formation, and thus proliferative vitreoretinopathy, be reduced but the hydrogel could also hold the re-attached the retina in place. This would drastically reduce post-operative recovery time.

The application of this research is not limited to the alleviation of current surgical complications. Current incarnations of retinal prosthetics have an increase in gliosis near to where the chip is in contact with the retina[32]. To deal with this problem, some have tried coating the pegs with carbon nanotubes[33]. Carbon nanotubes are hydrophobic which means they can easily penetrate the cell membrane[34, 35]. Because of this, even though a reduction in gliosis is seen, the cells end up dying. With proper application of our results to cover the chip with an appropriate gel, gliosis and cell death might be reduced. Electrical properties of such a gel would still need to be studied. Since the retina is a part of central nervous system (CNS) tissue, these results can be extrapolated for many other new central nervous system prosthetic and regenerative therapies as well.

CHAPTER 1

Müller Cell Expression of Genes Implicated in Proliferative Vitreoretinopathy is Influenced by Substrate Elastic Modulus

Introduction

The role of tissue stiffness has recently received increased recognition as a critical regulator of cell behavior[36-38]. In some cases such as development of liver fibrosis, changes in tissue stiffness precede and appear to contribute to subsequent dysfunction of hepatic cells[39]. The elastic modulus of the cells in adult mammalian retina has been found to vary between 200 Pascals (Pa) and 1000 Pa, and many pathologic processes in the retina lead to changes in stiffness of the local retinal tissue[40]. For example, it is well known that Bruch's membrane, immediately adjacent to the neurosensory retina, increases in stiffness by an order of magnitude with age[41]. Laser photocoagulation, retinal detachment, and retinal gliosis are likely to markedly alter the local elastic modulus

experienced by retinal cells. For this reason, we sought to determine the influence of substrate elastic modulus on Müller cells of the retina.

Müller cell morphology, propagation, and messenger RNA (mRNA) expression of select genes were studied utilizing fluorescence and atomic force microscopy (AFM) and quantitative real-time polymerase chain reation (qPCR) on a conditionally immortalized mouse Müller cell line (ImM10)[42] that was cultured on laminin-coated polyacrylamide substrates of varying elastic modulus. Particular attention was paid to the influence of substrate elastic modulus on extracellular matrix (ECM) gene expression and an 85 extracellular matrix gene array (SA Biosciences) was utilized to quantify gene expression.

Methods

Cell culture substrates were prepared on German glass coverslips (15 mm, Carolina Biological Supply) as described previously[36] according to the protocol of Pelham and Wang[43, 44], with the following modifications. Gels were prepared with 7.5% acrylamide and bisacrylamide (bis) ranging from 0.02 to 1.0%. The elastic moduli

of the gels were 500 Pa, 1000 Pa, and 5000 Pa, to model the elastic modulus range normally found in neural tissues[38]. Laminin-coated glass[45] was used as a control to model typical cell culture conditions. In order to obtain a wider range of substrate stiffnesses in the evaluation of substrate stiffness versus cell stiffness, cells were also cultured on gels with a stiffness gradient, which ranged from 300 Pa to 20,000 Pa[46]. The strategy for creating stiffness gradients has been previously published[46]. Briefly, gradient generators, for production of gradient gels, made from polydimethyl siloxane (PDMS) microfluidic channels were fabricated using standard photolithography techniques. The stiffness of polyacrylamide gels was tuned by varying the concentration of bisacrylamide at a fixed acrylamide concentration[47]. Three solutions with the same acrylamide (Bio-Rad, Hercules, CA) concentration but different N,N0-methylene-bisacrylamide (Bio-Rad) concentrations were injected into the gradient generator. Each solution had an acrylamide concentration of 8% and a 2,2-diethoxyacetophenone (Sigma 227102) photoinitiator concentration of 0.5%. The bisacrylamide concentrations of the three inlets were: 0.02%, 0.02%, and 1%.

During development of the technique, Fluorescein (Sigma F6377) was added to the 0.02% bisacrylamide solution to evaluate the gradient of bisacrylamide concentration upon polymerization. The solutions were then driven through the microfluidic channels by syringe pumps (Harvard Apparatus, Holliston, MA) at the same flow rate of 3 mL. Once the flow in the outlet channel reached a steady state, a UV light was shined on the outlet region for 8 min. The syringe pumps were stopped after the outlet region was exposed in the UV light for 10 s. Peeling off the polydimethal siloxane gradient generator results in the gel being adherent to the activated coverslip. The resulting gel, 1.8 mm in width and 2 cm in length, was immediately immersed in PBS buffer for 12 h to remove unreacted photoinitiators. Once the gradient polyacrylamide gels were fabricated, the stiffness across the gel was characterized using AFM. The gradual transition in bis-acrylamide concentration, which correlates with gel stiffness, was also evaluated by fluorescence.

Final gel thickness after polymerization was §100 µm. A bifunctional cross-linker (50 mM sulfo-SANPAH (Pierce) in 200mM HEPES, pH 8.5) was used to ligate laminin or collagen to the polyacrylamide gels.

Laminin (50µg of 1mg/ml natural mouse laminin in 5.95ml HEPES buffer, Invitrogen™) or Collagen (0.1 mg/ml rat-tail collagen, BD Bioscience, San Diego, CA) was applied to the gels and incubated for 2 hours at 37˚C for cross-linking. Gels were rinsed once with Eagle's minimal essential medium (EMEM) and incubated overnight in Eagle's minimal essential medium in a humidified 37˚C incubator. Three hours before plating the cells, Eagle's minimal essential medium was removed and replaced with culture medium.

The static elastic modulus of each polyacrylamide mixture was confirmed using a Perkin Elmer DMA 7e dynamic mechanical analyzer. Each mixture was polymerized in the rheometer and uniaxially compressed in a 30 mm diameter parallel-plate geometry with force applied from 0 to 15 mN at 1 mN/min. Samples were evaluated at 37˚C at 2 Hz, with the shear rate increasing from 0.1 to 100 s-1.

A conditionally immortalized mouse Müller cell line, ImM10[42] was utilized in these experiments. The ImM10 cell line was isolated from the retinas of prenatal day 10 mice that were heterozygous for the

“immortomouse” transgene (H-2Kb-tsA58) that encodes an interferon gamma (IFN-γ) inducible, temperature sensitive SV40 large T antigen[48].

When grown at 33ºC, cells are immortalized by induction of the T antigen with IFN-γ at 50 U/ml final concentration in the media. Following withdrawal of Interferon-γ, T-antigen production is stopped, and shifting the cells to 39ºC inactivates the remaining, temperature sensitive Tantigen, thereby releasing cells from immortalization.

ImM10 cells were plated at 10,000 cells/well in a 24-well plate and cultured at 5.5% CO2 in growth medium composed of 500 mL Neurobasal media, 10 mL of B27 supplements, 5 mL of 200 mM L-glutamine, with 2% heat-inactivated fetal bovine serum (FBS) and penicillin/steptomycin antibiotics (all from Invitrogen). When Interferon-γ was required, 500 mg of mouse recombinant Interferon-γ (Peprotech) was added to a final concentration of 50 U/ml. The cells were maintained with Interferon-γ in the media, at 33ºC. All experiments were performed in non-immortalizing conditions without Interferon-γ, at 39ºC. Cells were studied or RNA was harvested after

21 days. This length of time was selected in order to allow the cells to accommodate to the substrate that they were plated upon. It has been previously noted that Müller cells that had been cultured for at least 12 days modified their expression profile, upregulating expression of glial fibrillary acidic protein, sox2, cyclinD3, ceruloplasmin, and nestin and downregulating glutamine synthase, Kip1, Kir4.1, and acquaporin-1[49]. In addition, changes in contractility of Müller cells were previously noted on the time scale of 3 weeks[50]. The cells were not confluent at the time of examination and were at passage 10 through 21.

Atomic force microscopy measurements were performed according to a published protocol. Briefly, Müller cells on substrates were rinsed with phosphate buffered saline (PBS) and placed in serum-free Delbucco's modified eagle medium. Atomic force microscopy measurements were done with a DAFM-2X Bioscope (Veeco, Woodbury, NY) mounted on an Axiovert 100 microscope (Zeiss, Thornwood, NY) using silicon nitride cantilevers (196 μm long, 23 μm wide, 0.6 μm thick) with a pyramidal tip (when the cell is indented by 1 μm, the area of the indentation projected on the sample plane is 1.6

μm^2) for indentation. The spring constant of the cantilever, calibrated by resonance measurements, was typically 0.06 N/m (DNP, Veeco). To quantify cellular stiffness, the first 600 nm of tip deflection from the horizontal (Δd) were fit with the Hertz model modified for a cone[51]:

$$\Delta d = \frac{k}{4A} + \Delta z + \frac{1}{2}\sqrt{\left[\left(\frac{k}{A}\right)^2 + 4\frac{k\Delta z}{A}\right]} \text{ and } A = \frac{2}{\pi}\frac{E}{1-\nu^2}\tan(\alpha)$$

where k and Δz are the bending rigidity and the vertical indentation of the cantilever, E is the Young's modulus, α is the cone tip angle, and v the Poisson ratio. Young's modulus is the inverse ratio between the strain (Δz/z) applied to the material and the resulting stress. The Poisson ratio is defined as the ratio of compressional strain in the direction normal to the applied stress and the extensional strain in the direction of the applied stress and is taken to be 0.5 for all samples. To determine cell stiffness, atomic force microscopy measurements were made on single cells by indenting on three positions of the peripheral cell body within a period of ~30 minutes. The average elastic modulus for each condition was calculated by averaging the three measurements for each cell followed by averaging all obtained values. At very large indentation, it is possible that the tip can rupture

the cell membrane. However, small indentations will not lead to cell rupture. For this reason, we only indented the Müller cells by approximately 1 µm, where the possibility of the tip penetrating the cell membrane is very low. Publications by the investigators and others have previously utilized this atomic force microscopy system reproducibly to obtain data. Moreover, we also monitor the indentation process using an optical microscope and did not observe changes in cell morphology after the atomic force microscopy measurements.

It has been previously shown[25] that atomic force microscopy measurements will be influenced by the underlying substrate when the indentation is larger than 10% of the sample thickness. Therefore, it is likely that the stiffness will be influenced by the substrate stiffness if the atomic force microscope indentations were taken over the cell lamelipodia, whose thickness is often less than a micrometer. Being aware of this issue, and specifically seeking to avoid the influence of the substrate, we obtained measurements on the peri-nuclei regions of the cells. The cell thickness in these regions is on the order of a few micrometers, significantly larger than the thickness of a

lamelipodium. To verify the appropriateness of this technique, we plotted atomic force microscope cantilever deflection as a function indentation as well as cell stiffness as the indentation depth increases from 200 nm to 1 μm. The cell stiffness values did not vary significantly with the indentation depth. (please see Supplementary Material, Figures 1, and 2). In order to evaluate cell morphology, the cells were fixed with 4% paraformaldehyde and prepared for dual immunofluorescence and epifluorescence microscopy. Cells undergoing rhodamine-phalloidin (Invitrogen™) staining were treated according to a standard protocol with nuclear counterstaining. Cells were imaged using an inverted Olympus microscope (IX71; Olympus, Tokyo, Japan) equipped with a monochrome, cooled CCD digital camera (Rolera-XR; Q-Imaging, Surrey, BC, Canada). Images were quantified for average spread area utilizing NIH Image, with at least 10 cells per high-powered field analyzed. Propagation was measured in triplicate utilizing a hemocytometer and Trypan blue stain. Less than 1% of cells counted were non-viable.

Gene expression was analyzed by quantitative real-time polymerase chain reaction using the Stratagene MX3005P real-time polymerase

chain reation system and the SA Biosciences extracellular matrix and adhesion molecules real-time PCR array (which is composed of 85 genes important for cell-cell and cell-matrix interactions plus 5 housekeeping genes for normalization, controls for genomic DNA contamination, and positive and negative controls). Total RNA was isolated from cells using affinity columns (RNeasy, Qiagen). Briefly, cells were lysed in a guanidine hydrochloride buffer, loaded onto affinity columns, washed, and eluted in RNAse free water (RNeasy, Qiagen). Samples were quantified by 260 nm absorbance using spectrophotometry (Nanodrop) and stored at -80˚C. First strand cDNA was synthesized using reverse transcriptase (RT2 First Strand Kit, SAB Biosciences) according to the manufacturer's instructions. The RT2 kit uses a combination of random hexamers and oligo-dT to prime the reverse transcriptase reaction and utilizes a proprietary procedure to eliminate any contaminating genomic DNA from the reactions. Master mix, containing 12.5 µL cDNA was added to each well of a polymerase chain reaction array (extracellular matrix and adhesion molecules PCR Array, PAMM-013, SA Biosciences). Cycling conditions followed manufacturer's recommendations and

performed on a real-time polymerase chain reaction instrument (Mx3005p, Stratagene). Web-based analysis software (SABiosciences) was used to analyze the results of the experiments. The proteins of greatest interest in this study are secreted, and thus the protein cannot be obtained purely from cell lysates and the proteins are known to degrade rapidly, producing broad bands on western blotting. For this reason, mRNA was quantified as an indirect measure of protein production.

Descriptive statistics including mean, median, and standard deviation were calculated. Linear regression was used to analyze atomic force microscopy elastic modulus measurements. Analysis of variance (ANOVA) was used to assess the relationship between the genes expressed.

Results

As Müller cells were grown on their separate substrates, morphological changes became readily apparent. Cells grown on the stiffer substrates such as glass and 5000 Pa gels (Fig. 1A,B) had a much larger spread area ($p=0.0428$) along with being more

individuated than the corresponding cells on softer substrates (Fig. 1C,D).

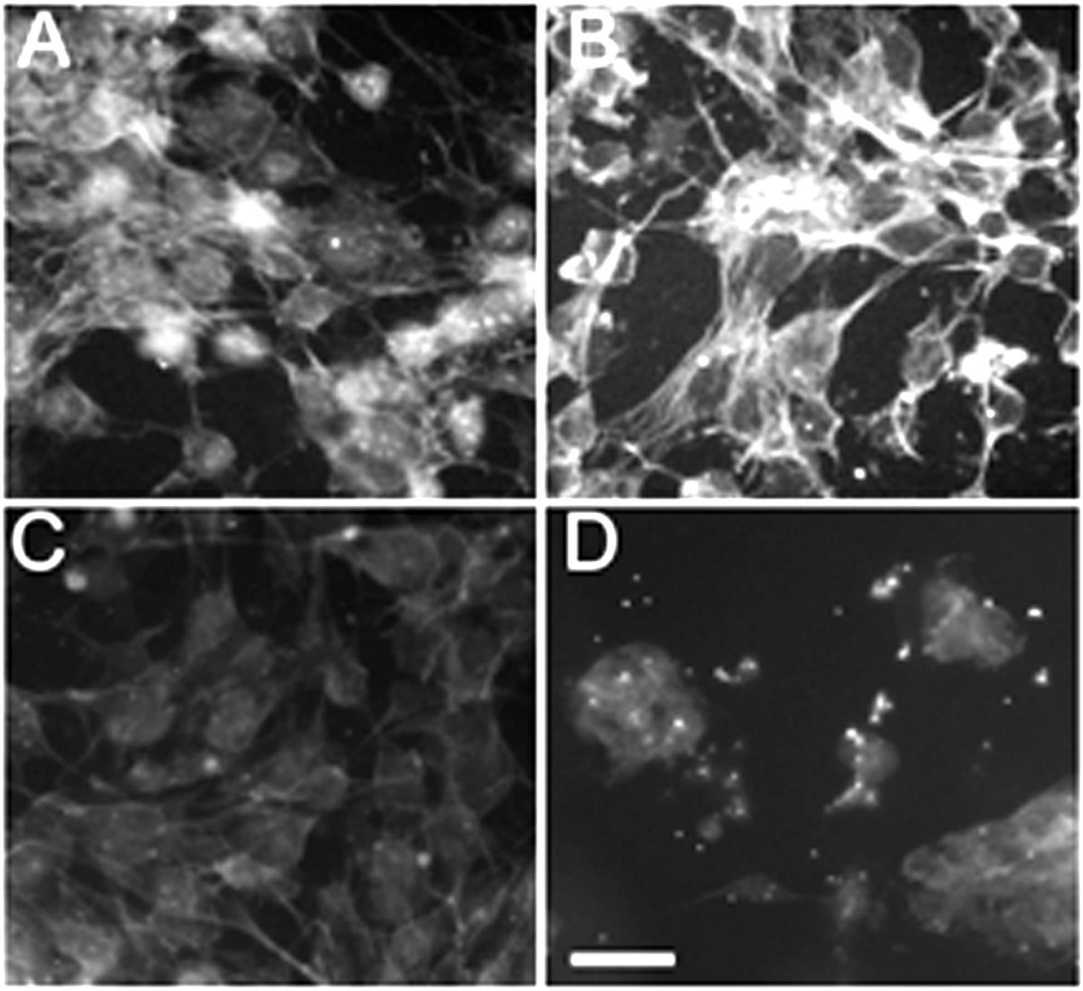

Figure 1.1: Photomicrographs of rhodamine-phalloidin-stained Müller cells, with nuclearcounterstaining, on laminin-coated substrates. Cells grown on laminin-coated glass (upper left) and 5000 Pa substrates (upper right) display prominent stress fibers. Cells on 1000 Pa (lower left) and 500 Pa substrates (lower right) demonstrate very minute levels of rhodamine-phalloidin staining as well as a more spherical morphology. Scale bar= 100 microns.

These changes are less apparent on collagen-coated substrates (Fig. 1.2) but are still present with an approximate two-fold increase in spread area across the range tested (Fig. 1.3).

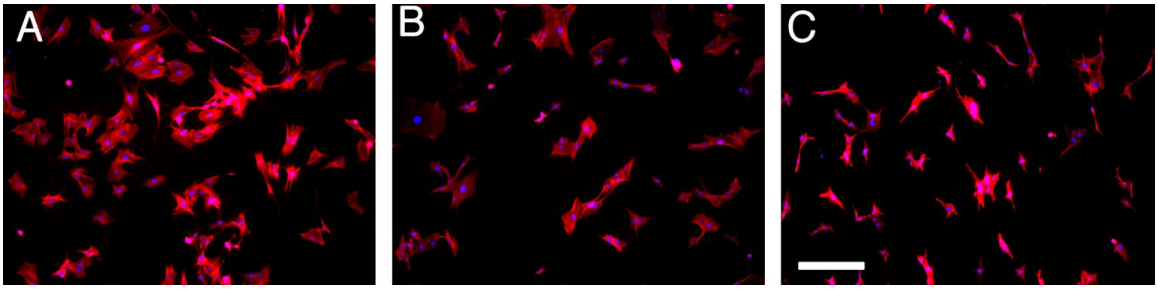

Figure 1.2: Images (from left to right) of Müller cells cultured on collagen-coated plastic and collagen-coated gels of stiffness 1500 Pa, and 500 Pa. Cells were stained with Texas Red-phalloidin with nuclear counterstaining. Note the transformation of cell shape from more polygonal to elongated with a decrease in the number of stress fibers and that differences in basement membrane protein (Laminin in Figure 1 versus Collagen in Figure 2) significantly alter cell morphology. Scale bar= 200 microns.

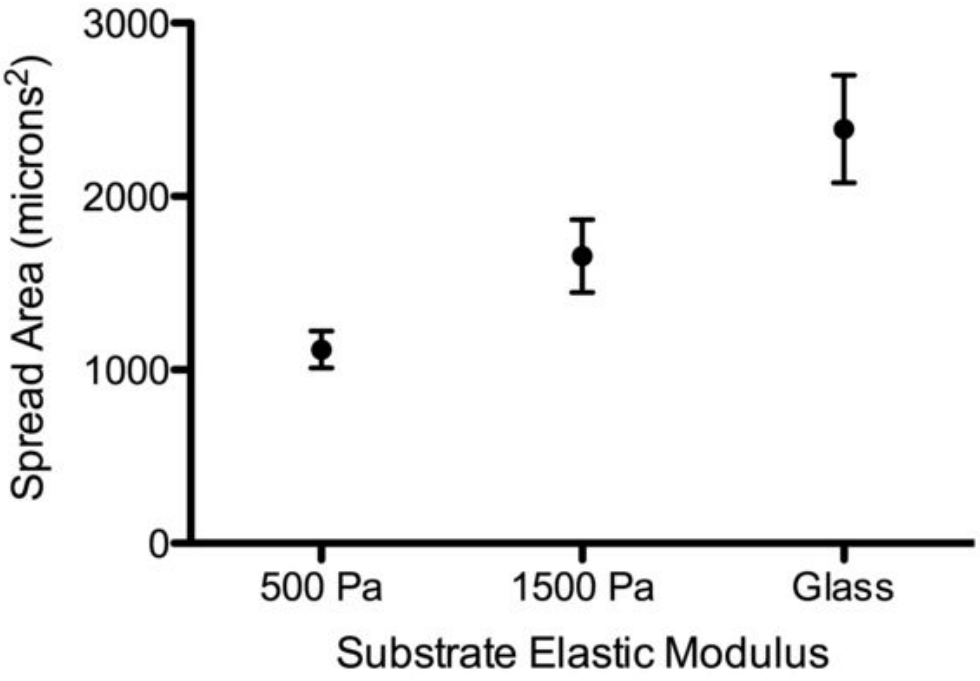

Figure 1.3: Müller cell spread area (square microns) plotted as a function of substrate stiffness (p=0.0428) on collagen-coated substrates.

Using phalloidin staining, prominent stress fibers are apparent in the larger cells, but not in cells with smaller adherent areas on softer gels. Cytoskeletal rigidity is shown by atomic force microscope measurements on the cortical actin in the cells, and demonstrates a linear increase in cell stiffness with respect to substrate stiffness up to 2000 Pa (Fig. 1.4), followed by an apparent saturation of cell stiffness as the matrix stiffness is further increased.

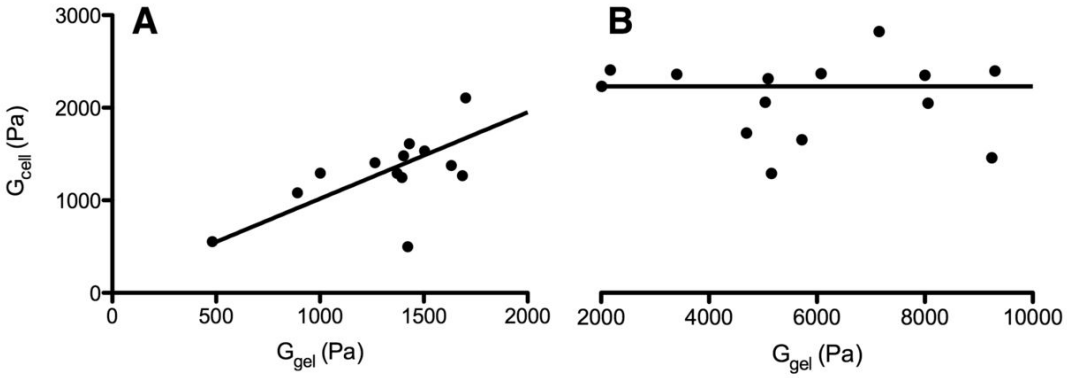

Figure 1.4: Atomic force microscopy evaluation of the cortical actin elastic modulus as a function of substrate elastic modulus in cultured Müller cells. Below 2000 Pa (left), the cortical actin elastic modulus increases linearly with substrate elastic modulus. Above 2000 Pa (right), the cortical actin elastic modulus remains nearly constant (the horizontal line is included to guide the eye). Linear regression on data below 2000 Pa results in a best-fit slope of (0.933±0.216) with a y-intercept of (84.48±320) ($p=0.0008$, $R2=0.98$).

Propagation of glia may be important in proliferative vitreoretinopathy because of the extensive gliosis that develops in this condition. Cells on harder substrates propagated more quickly than those on softer substrates, with cells on 1000 and 500 Pa being statistically indistinguishable (Fig. 1.5). The results for day 12 on the glass substrate do not demonstrate exponential growth because of near-confluence of the cells.

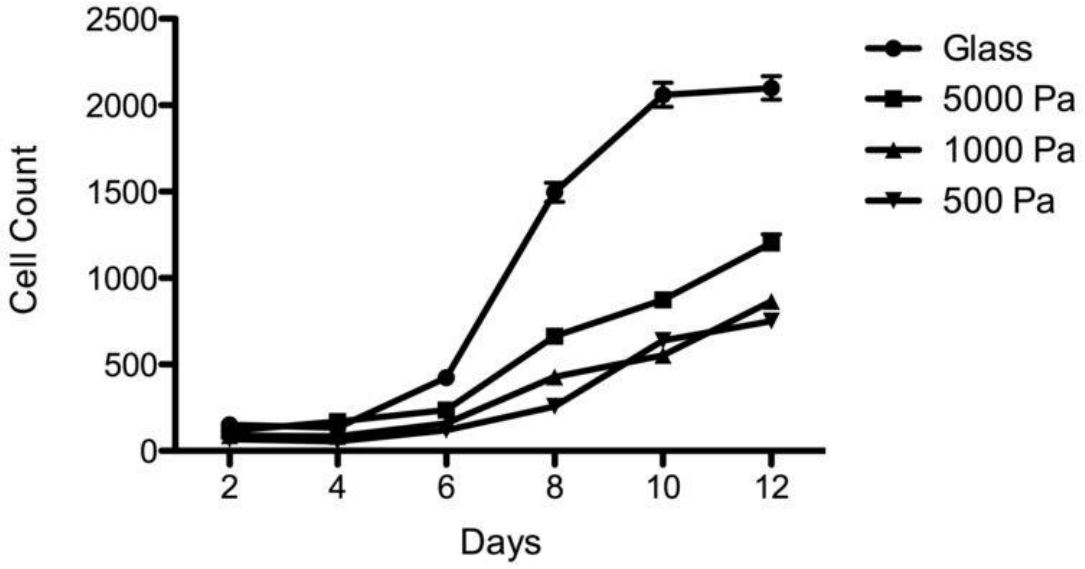

Figure 1.5: Müller cells, quantified using a hemocytometer, increased in number more rapidly on firmer substrates. There is a transition point between 1000 Pa and 5000 Pa, such that cells on firmer substrates propagation more rapidly. The results for day 12 on the glass substrate do not demonstrate exponential growth because of near-confluence of the cells.

Polymerase chain reaction results were obtained from preloaded plates for extracellular matrix proteins. From these results, it was observed that there is a large, nonlinear upregulation of connective tissue growth factor (CTGF) as well as tenascin-C (TNC) (Fig. 1.6).

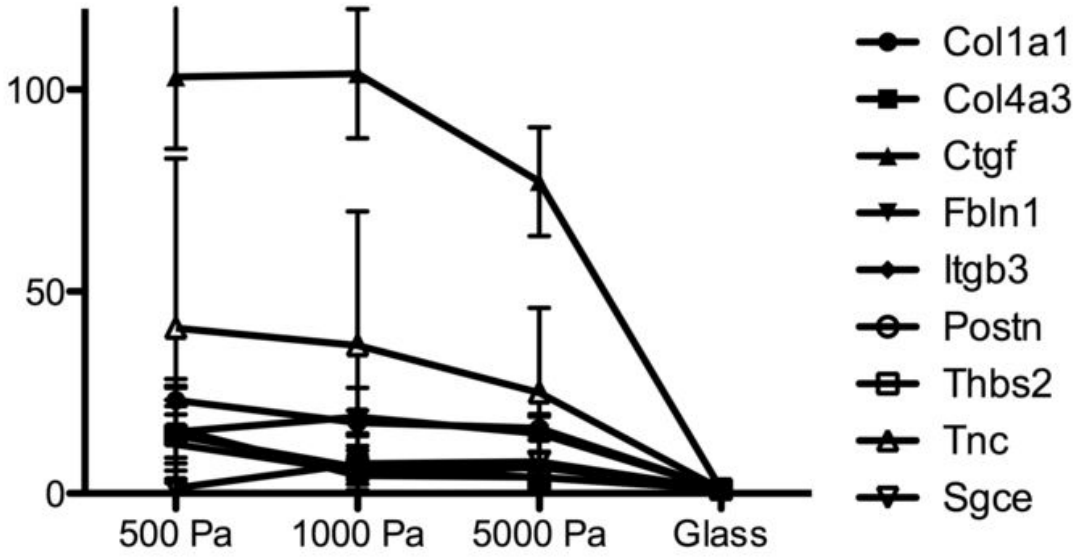

Figure 1.6: mRNA expression, quantified using real-time polymerase chain reaction arrays on cells grown on substrates of different elastic modulus. Note the orders-of-magnitude change in expression as a function of substrate elastic modulus. Genes plotted with solid lines demonstrate statistically significant changes with regression analysis (collagen 1 alpha 1 (Col1a1) p=0.001, collagen 4 alpha 3 (Col4a3) p=0.05, connective tissue growth factor (Ctgf) p=0.05, tenascin-C (Tnc) p=0.035). Genes plotted with dashed lines were not found to have statistically significant changes.

Connective tissue growth factor was shown to have a two order of magnitude increase on softer substrates, with respect to glass, ($p=0.05$) with tenascin-C having a 40-fold increase ($p=0.035$). Similarly, both collagen type 4 alpha 3 and collagen type 1 alpha 1 increased with decreasing substrate elastic modulus ($p=0.05$ and $p=0.001$ respectively, 500 Pa vs. glass). In contrast to these changes in extracellular matrix components, there was no significant trend observed in matrix metalloproteinase expression 10.

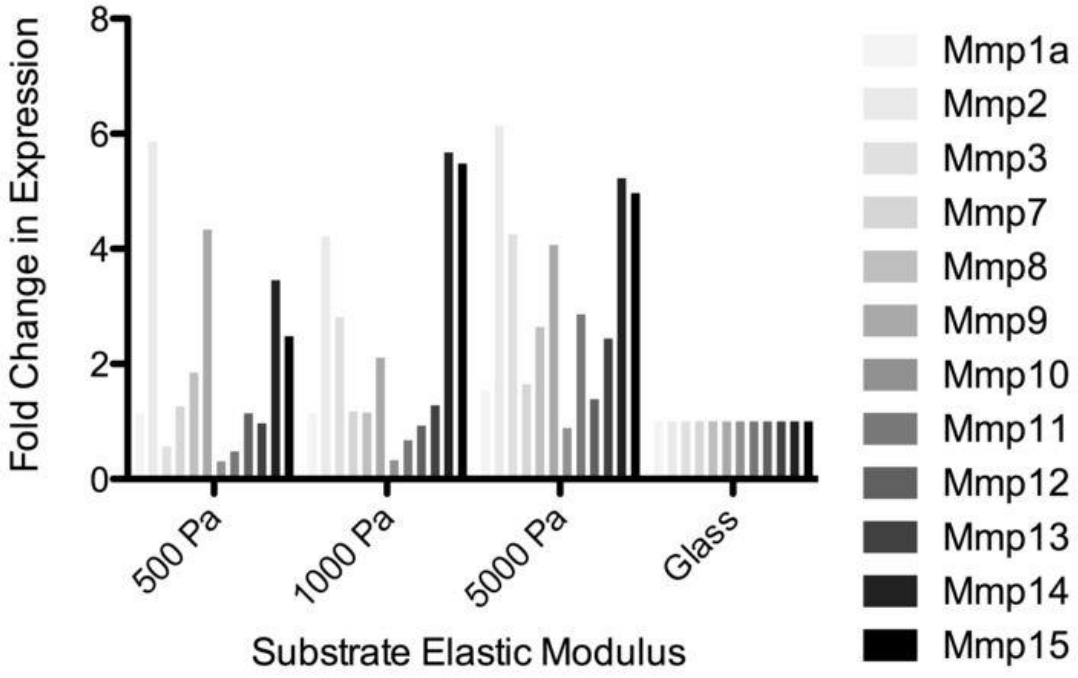

Figure 7. Matrix metalloproteases gene expression using real-time PCR arrays on cells grown on substrates of different elastic modulus. There does not appear to be any dependence of matrix metalloprotease expression on elastic modulus, but a baseline expression is present.

Discussion

The effective stiffness of the retina can be altered through a variety of pathological processes. Stiffening of the retina occurs with age[41] and retinal gliosis. The local elastic modulus in the retina is likely to be decreased in conditions such as retinal photocoagulation with coagulative necrosis and retinal detachment. In particular, it is known from thermodynamic calculations, that supported membranes (i.e., attached retina) have a markedly greater stiffness than unsupported membranes[52].

Prior studies, utilizing similar techniques on different cell types[36, 38, 39] report changes in morphology that are consistent with the current findings, in a wide variety of cell types. This suggests that changes in gene expression may be influenced by changes in cell shape and morphology, as has been found in many cell types[36, 38, 53].

Connective tissue growth factor (CTGF), the product of the gene most strongly affected by substrate stiffness, plays numerous roles in pathologic conditions of the retina including proliferative vitreoretinopathy[54], age-related macular degeneration[55, 56], and

diabetic retinopathy[56, 57]. Not only is connective tissue growth factor thought to be the major mediator of retinal fibrosis in the presence of transforming growth factor-β[54], (which is present at significant levels in the vitreous fluid), it is necessary for diabetes-induced basal lamina thickening[57].

Histologically, the immunoreactivity of proliferative vitreoretinopathy (PVR) membranes to connective tissue growth factor is known to increase with the stage of proliferative vitreoretinopathy[58]. Connective tissue growth factor induces fibronectin, laminin, and matrix metalloproteinase-2 (MMP-2) expression in retinal pigment epithelium cells, is strongly present in Bruch's membrane, including basal deposits and drusen[55], and stimulates migration of retinal pigment epithelial cells[56]. Finally, connective tissue growth factor stimulates the synthesis of fibronectin by hyalocytes and retinal pigment epithelial cells[59] and hypoxia is known to increase the expression of connective tissue growth factor, collagen IV, and fibronectin[60]. Based upon the prior literature, reviewed in the manuscript, the cultures were performed for 21 days prior to analysis. For this reason, there is much greater heterogeneity in the distribution

of the cells. Cells that become confluent may respond differently to mechanical stress than non-confluent cells. For this reason, analysis of confluent monolayers was avoided.

Our finding that expression of connective tissue growth factor by Müller cells is markedly increased on soft substrates is thus notable, because it provides a complementary, physical mechanism whereby connective tissue growth factor can be regulated in pathological conditions. For example, it might be expected that, after cryotherapy or photocoagulation and resulting tissue necrosis, nearby Müller cells would upregulate their expression of connective tissue growth factor. In addition, when embedded in a detached (and thus soft) retina, with no underlying substrate, Müller cells would be expected to upregulate their expression of connective tissue growth factor.

Recently, the activity of the transcription regulators YAP/TAZ (Yes-associated protein and transcriptional coactivator with PDZ-binding motif, also known as WWTR1) has been found to be regulated by substrate stiffness to a degree comparable to short interfering RNA (siRNA) mediated Yes-associated protein/taffazin depletion[61]. Yes-

associated protein/taffazin was found to be predominately nuclear in spread cells and on hard substrates, while this pair was predominately cytoplasmic on soft substrates or when cells were confined to small islands. In a bioinformatic analysis on genes differentially expressed in mammary epithelial cell (MECs) grown on substrates of high versus low stiffness, connective tissue growth factor was found to be one of the genes most strongly regulated by Yes-associated protein/taffazin[62]. This finding was confirmed in a variety of cell types, including MDB-MB-231 (a mammary adenocarcinoma cell line) and HeLa cells (a cervical cancer cell line). The change in nuclear localization was found to be related to cell geometry and cytoskeletal tension, independent of cell-cell contact, and independent of the Hippo pathway, within which Yes-associated protein and taffazin are the nuclear transducers. Our findings of differential regulation of connective tissue growth factor on substrates of varying elastic moduli suggest that Yes-associated protein/taffazin may play a critical role in gliotic changes commonly present in vitreoretinal disease and may provide therapeutic 12 targets for these blinding conditions.

Tenascin-C (TNC) is an extracellular protein that is known to modulate cell-matrix interactions[63] and can either contribute to, or inhibit[64], integrin-mediated spreading of cells. Tenascin-C has been noted to be differentially regulated in fibroblasts on matrixes of varying stiffness and it has been hypothesized that its promoter contains a stretch-responsive enhancer element[65]. In vivo, at the myotendinous junction, its expression has been found to be strongly regulated by mechanical loading[66].

Consistent with our findings, tenascin-C has previously been found to be non-linearly and markedly upregulated with injury in a rat model of elevated intraocular pressure[67] and has also been identified[68] in the schisis cavities of patients with congenital x-linked retinoschisis. Given our results, these prior findings are likely to be related to changes in the mechanical stiffness of optic nerves that have been injured by an acute episode of glaucoma and of retinas that contain a schisis cavity.

Expression of multiple collagen genes can be regulated by mechanical stress, with the particular collagen involved determined

by cell type[65]. Thus, it is not surprising that we find the expression of collagens (Col1a1 and Col4a3) influenced by stiffness. Matrix metalloproteinases are expressed in Müller cells, but do not depend upon substrate modulus.

Weaknesses of this study include the use of a cell line that may not be representative of in vivo conditions. In addition, for many of the measurements, evaluation of the cells was performed at one time point, a time at which Müller cells were known to have changed their expression profile. This does not allow evaluation of more transient changes in the Müller cells as a function of substrate stiffness. Such evaluation would likely require “equilibration” of the cells either in vivo (for primary cells) or at a physiological substrate stiffness (such as a 1000 Pa).

In summary, many surgical interventions and pathologic conditions in retinal disease can result in changes in the elastic modulus of ocular tissue. Examples include photocoagulation and cryosurgery, that can result in initial necrosis and decrease in retinal elastic modulus and aging and traction, which can result in increases in retinal and

basement membrane elastic modulus. Necrotic tissue, immediately after coagulative necrosis, will be soft, given the aggregation of cytoskeletal elements and the well-known formation of blebs in the plasma membrane while the subsequent longer-term tissue stiffness is currently a subject of study.

These physical changes in tissue can have marked and direct influence upon genes, such as connective tissue growth factor and tenascin-C, which are known to play a key role in pathologic conditions, such as proliferative vitreoretinopathy. Our findings suggest that the Yorkie-homologues and transcriptional regulators Yes-associated protein and taffazin may provide a therapeutic target for the treatment and prevention of gliotic diseases of the retina and optic nerve.

CHAPTER 2

Time Related Response of Connective Tissue Growth Factor Expression in Müller Cells to Varying Elastic Moduli

Introduction

As the concept that extracellular matrix stiffness plays a role in the development and genetic response of cells[36-38] has increasingly become accepted, research in this field has diversified. Recent work with epithelial cells has shown that the area to which a cell is constrained can be just as important as the underlying stiffness[61]. As a cell's spread area decreases, the expression of connective tissue growth factor (CTGF) is altered[61]. Not only this, but the Yes-associated protein/taffazin protein complex is located in different locations in the cell (cytoplasmic or nuclear), depending upon substrate stiffness or constrained area[61].

The elastic modulus of the cells in adult mammalian retina has been found to vary between 200 Pascals (Pa) and 1000 Pa, and many pathologic processes in the retina lead to changes in stiffness of the

local retinal tissue[40]. For example, it is well known that Bruch's membrane, immediately adjacent to the neurosensory retina, increases in stiffness by an order of magnitude with age[41]. Retinal detachments and laser photocoagulation can also markedly affect the stiffness experienced in the retina. In a previous paper, it was shown that Müller cells increase in spread area with increased substrate stiffness, as is seen in epithelial cells[69]. Increased substrate stiffness was also shown decrease in mRNA expression of tenascin-C (TnC) and connective tissue growth factor[69], this is in opposition to what was found in other works[61]. Because of this, we used the same conditionally immortalized Müller cell line[42] to determine the changes in protein expression of both tenascin-C and connective tissue growth factor. Cells were grown on polyacrylamide substrates ranging from 500 to 5000 Pa and protein expression was determined by western blot and enzyme-linked immunosorbant assay. Immunohistochemical imaging was also performed to investigate how the Yes-associated protein/taffazin complex localized within these cells.

Materials and Methods

Cell Culture

Conditionally immortalized Müller cells (ImM10)[42] were plated on laminin-coated polyacrylamide gels[43, 44] or glass substrates and maintained in cell culture at 5.5% CO_2. After plating, adherent cells were maintained for 24 days at 37^{o}C in growth medium under nonimmortalizing conditions (Neurobasal with 2% fetal bovine serum (FBS), 2% B27 supplements, 1% 200mM l-glutamine, and 1% antibiotics (Gibco/Invitrogen)) with media changes at 3 day intervals. For growth under immortalizing conditions, media was supplemented with mouse recombinant interferon-γ (PreproTech; Rocky Hill, NJ) at 50 U/mL. For maintenance and subsequent analyses, cells were grown on uncoated tissue culture dishes unless otherwise stated.

Substrate Preparation

Glass coverslips were coated with a drop of 3-aminopropyltrimethoxysilane spread evenly on the surface. Each coverslip was then washed with deionized water, placed into foil packets, and autoclaved. Once autoclaved, the coverslips were

transferred to a petri dish containing 0.5% gluteraldehyde (70% stock solution, Sigma) in phosphate buffered saline and left to incubate for 30 minutes at room temperature. This was followed by 5, 10 minute washes in autoclaved deionized water. After the last wash, the coverslips were laid out onto a piece of autoclaved foil to dry.

Gel Formation

Three different stiffnesses of gel were prepared: 5000, 1000, and 500 Pa. Concentrations of acrylamide and bisacrylamide were prepared and measured using atomic force microscopy and rheometry. Mixtures were made up for each stiffness corresponding to the atomic force microscopy results (5000 Pa: 7.5% acrylamide 0.5% bisacrylamide; 1000 Pa: 7.5% acrylamide 0.2% bisacrylamide; 500 Pa: 7.5% acrylamide 0.1% bisacrylamide). These mixtures were then filtered by use of a syringe and 5.9 µL was placed onto each coverslip, which was then covered with a second coverslip that had been treated with Sigmacote (Sigma, St Louis, MO) to ensure even coverage. The set gels were placed in a 24-well plate and washed with HEPES before being treated with a 0.5 mg/mL solution of SULFO-SANPAH (Sigma). This was then activated under UV light for

10 minutes before three more washes in preparation for the laminin. A 1% laminin solution was prepared in HEPES (Sigma), 200 µL of this solution was then placed into each well of the 24-well plate and allowed to incubate at 37^{o}C for 4 hours. Once this was done, all liquid was removed and replaced with growth medium and placed back at 37^{o}C for 15 minutes before the cells were added.

Immunohistochemistry

For immunostaining, tissues or cells were fixed in 4% paraformaldehyde for 10 minutes at 37^{o}C. Samples were washed in PBS, incubated in PBS containing 0.5% Triton X-100 (10 minutes), and blocked with PBS containing 10% normal goat serum/0.5% Triton X-100/1% fish gelatin/5% bovine serum albumin for 1 hour. Primary antibody to Yes-associated protein/taffazin complex was diluted 1:200 and applied for 2 hours at room temperature with rotation. Secondary antibody conjugated to Alexa Fluor 555 (Gibco/Invitrogen) was diluted 1:500 and incubated 2 hours at room temperature. Samples were then mounted using Slowfade Gold with DAPI (Invitrogen). Specificity of labeling was confirmed by omitting primary antibody or by substituting normal serum for the species used to

generate the primary antibody. Immunostained cells were imaged with an inverted microscope (IX71; Olympus, Tokyo, Japan) with monochrome, cooled CCD digital camera (Rolera-XR; Q-Imaging, Surrey, BC, Canada).

Western Blot Analysis

ImM10 cells in growth medium were grown on 35mm plates for 28 days at 37^{o}C, with media changes every 3 days. Cells were harvested using RIPA buffer (Sigma) and scraped from the substrate using a rubber tipped cell scraper and transferred to a microcentrifuge tube. The cells were then lysed by being spun at 14,000g for 15 minutes and the supernatant containing the cell lysate was transferred to a fresh tube. Cell lysates were quantified by bicinchoninic acid assay (BCA-1; Sigma), diluted in Laemmli buffer (2x final concentration) and were loaded at 30 µg/lane onto duplicate polyacrylamide gels (Bio-Rad, Hercules, CA). After electrophoresis at 200 V, proteins were transferred onto nitrocellulose (NT8017; Sigma) by electroblotting and processed for immunodetection using anti-tenascin-C antibodies (Synaptic Systems) at 1:250 and enhanced chemiluminescence (Amhersham Biosciences, Pittsburgh, PA).

Duplicate gels, run in parallel and stained (Gel-Code Blue; Pierce, Rockford, IL), were used to compare protein loading.

Enzyme-linked Immunosorbant Assay

Enzyme-linked immunosorbant assay was performed using specialized enzyme-linked immunosorbant assay plates prepared with antibodies to mouse connective tissue growth factor (USCN, Wuhan, China) and according to the manufacturer's instructions. ImM10 cells were cultured in 35mm dishes on the four different substrates for 24 days with complete removal of the supernatant every 3 days. The supernatant was transferred to a microcentrifuge tube and frozen at -80^{o}C until all samples were collected. All substrates were collected in triplicate and diluted 1:20 in deionized water before use in assay. For the non-immortalized cell conditions, the cells were grown on 1000 Pa gels at 37^{o}C for 14 days before being transferred to the different substrates.

Results

The Western blot for renascin-C showed a 3.5 fold upregulation of protein on the 500 Pa and a 3.2 fold increase on the 1000 Pa, these

values were taken relative to the 5000 Pa gel. This progression has a p-value of 0.0024 when using the analysis of variation to account for the gradation in conditions.

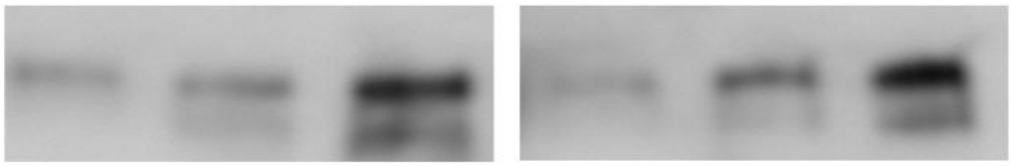

Figure 2.1: Western blot for tenascin-C in duplicate; from left to right cells from 5000 Pa gel, cells from 1000 Pa gel, and from 500 Pa. The Western blot for tenascin-C showed a 3.5 fold upregulation of protein on the 500 Pa and a 3.2 fold increase on the 1000 Pa, these values were taken relative to the 5000 Pa gel. This progression has a p-value of 0.0024 when using the analysis of variation to account for the gradation in conditions. Second set is a repeat. Cropped to remove intervening ladder and blot for cells grown on plastic.

The enzyme-linked immunosorbant assay for connective tissue growth factor showed a surprising trend in the time regulation of expression. The data show two distinct peaks in expression. The harder substrates, glass and 5000 Pa, both have a peak at day 15 in culture while the softer substrates have a peak at day 21.

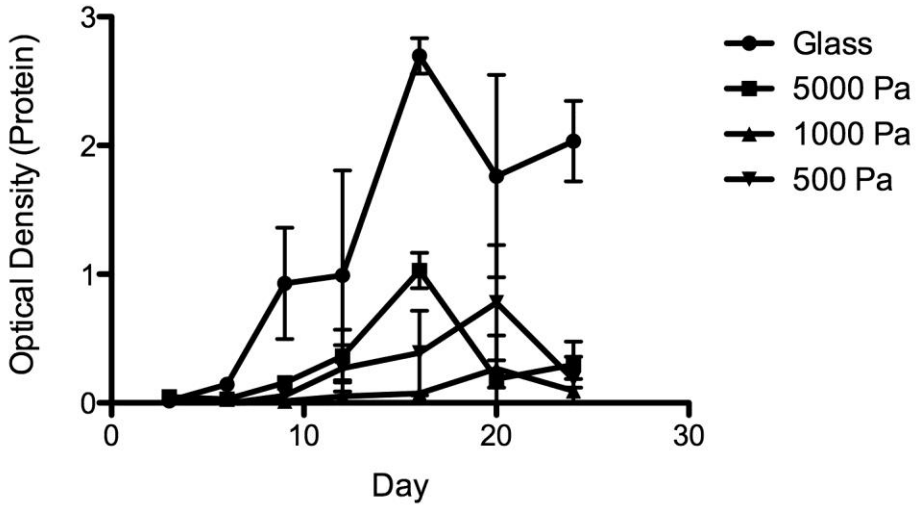

Figure 2.2: Enzyme-linked immunosorbant assay for connective tissue growth factor showing distinct peaks, the harder substrates show an earlier peak at day 15 while the 500 and 1000 Pa gels show a peak at day 21. Using two-way ANOVA the elastic modulus was determined to have a p-value of 0.0011, while the time component has a p-value<0.0001.

For staining for Yes-associated protein/faffazin, the cells were fixed after 15 days in culture and after 21 days in culture to correspond with the peaks seen in the enzyme-linked immunosorbant assay. The images show a transition from cytoplasmic to nuclear in correspondence with a peak in protein production. The proteins Yes-associated protein and taffazin were found to be predominantly cytoplasmic at the time of peak expression and to be nuclear while connective tissue growth factor expression is quiescent.

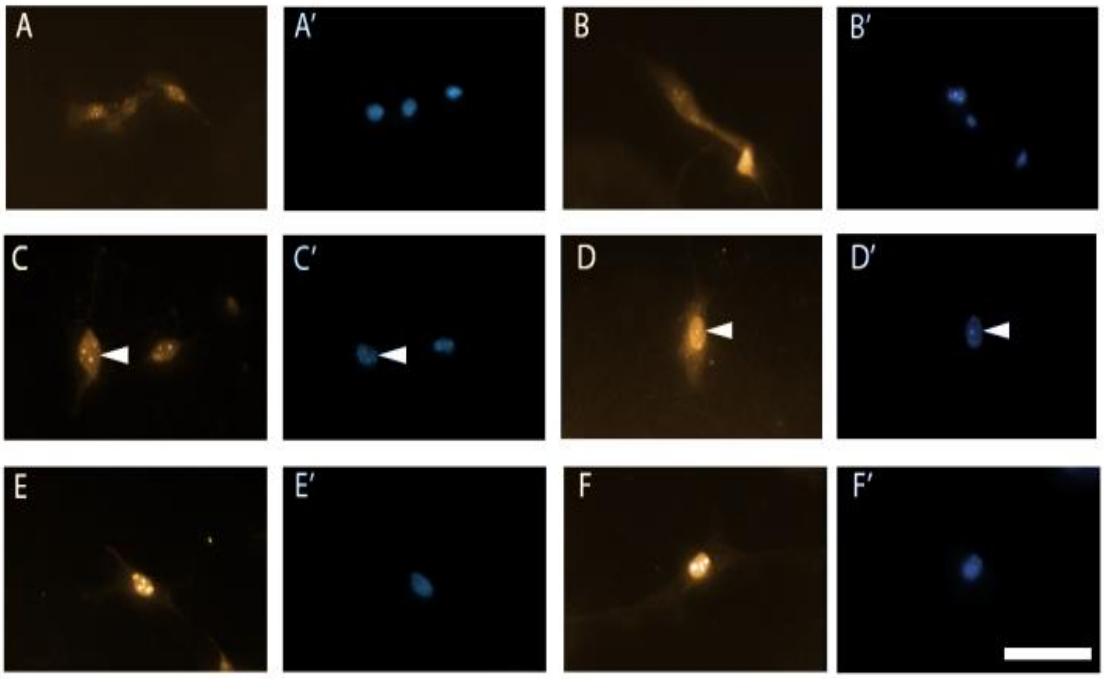

Figure 2.3 A-F': Unprimed letters are the staining for Yes-associated protein (YAP) primed letters are nuclear staining. 15 days in culture showing a larger cytoplasmic localization of YAP on 500 and 1000 Pa gel (A, B, C, D) with corresponding Hoechst staining of DNA (A', B', C', D'). 5000 Pa gels (E, F) show a greater concentration of stain in the nucleus, demonstrated by overlapping Hoechst stain (E', F') Scale bar: 50 microns.

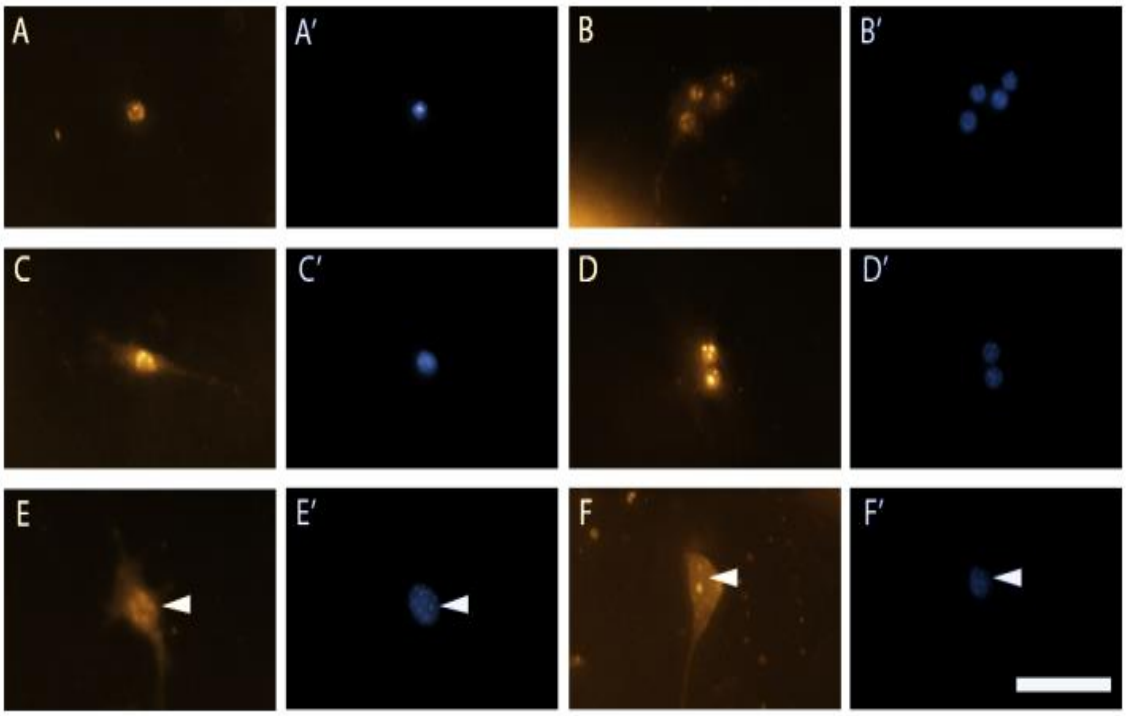

Figure 2.4 A-F': Unprimed letters are the staining for Yes-associated protein (YAP) primed letters are nuclear staining. 21 days in culture showing a larger nuclear localization of YAP on 500 and 1000 Pa gel (A, B, C, D) highlighted by corresponding Hoechst staining of DNA (A', B', C', D'). 5000 Pa gels (E, F) show a greater concentration of stain in the cytoplasm; Hoechst stain (E', F') included showing nuclear location. Scale bar: 50 microns.

Discussion

The occurrence of two separate peaks, and not a range, in the enzyme-linked immunosorbant assay data is in concordance with our data on the cytoskeletal stiffness of cells, determined by atomic force microscopy, when grown on different substrates. In the enzyme-linked immunosorbant assay results, it was shown that there were two distinct regions. First, up to 1500 Pa, the cellular stiffness rose linearly with substrate stiffness. Secondly, for substrate stiffness above 1500 Pa, there was no increase in cellular stiffness. Both the atomic force microscopy and enzyme-linked immunosorbant assay experiments have demonstrated a distinct change in cellular behavior when grown on substrates stiffer than the natural environment of the cells. This could even suggest the ability to “tune” cellular conditions and growth patterns by a relatively small change in the surrounding environment. This also has the converse explanation that even small changes to the natural elastic moduli of tissues in the body can have significant effects, perhaps as large a change as induced by implants and scar tissue.

The presence of two distinct states also corresponds to the findings by Dupont on the Yes-associated protein/taffazin protein pathway, in which the protein either is cytoplasmic or nucleic[61]. This could also aid in determining the transition point for when the protein complex changes from cytoplasmic. While our results varied slightly from what was found by Dupont[61], the different time points shed more light on the pathophysiology. The transition from one state to another occurs around peak expression. This suggests that the Yes-associated protein/taffazin complex plays a role in the negative feedback loop of transcription, at least in conjunction with connective tissue growth factor. The complex is cytoplasmic around the time the protein is being expressed and appears in the nucleus when transcription becomes quiescent. Tenascin-C has a limiting factor on extracellular matrix binding which would limit the spread area of the cells on the softer substrates. This outcome would correspond with why Yes-associated protein/taffazin is cytoplasmic (inactive) in cells on stiff substrates but with small binding areas, as both situations contribute to a more spherical cell shape by preventing adhesion to extracellular matrix proteins which are at a distance. Essentially, the cells on softer

substrates are creating natural “fibronectin islands” discussed in the Dupont paper[61].

Chapter 3

The Influence of Substrate Elastic Modulus on Retinal Pigment Epithelium Cell Phagocytosis

Introduction

The most common form of age-related macular degeneration is the non-exudative, or dry form. Retinal pigment epithelial (RPE) cells are thought to play an important role in the development of dry macular degeneration because they are located on Bruch's membrane, directly under the retina and provide metabolic support for the photoreceptor cells (rods and cones)[70]. As patients age, retinal pigment epithelial cells have been found to undergo structural changes including accumulation of the pigment lipofuscin, loss of melanin, and accumulation of drusen on Bruch’s membrane[71].

The process of non-exudative macular degeneration may be initiated by the failure of retinal pigment epithelial cells to phagocytose the debris from the outer segments of photoreceptors[71]. This results in an accumulation of drusen (deposits of lipids and calcium[72]) adjacent to the basement membrane of retinal pigment epithelial

cells[73]. The buildup of drusen may lead to atrophy of the retinal pigment layer below the retina and eventually cause vision loss through loss of photoreceptors in the central part of the macula.

The elastic modulus of the environment in which a cell exists has recently been shown to influence cell processes such as proliferation[37], motility[43], and gene expression[44]. Bruch's membrane is known to increase in stiffness by an order of magnitude (from 1,000 Pa to 10,000 Pa) with age[41]. We hypothesize that retinal pigment epithelial cells will demonstrate decreased phagocytosis on stiffer substrates. To better understand whether phagocytosis is influenced by substrate stiffness, we investigated the influence of substrate elastic modulus on phagocytosis in the retinal pigment epithelium cell line ARPE-19.

Methods and Materials

Preparation of Glass Coverslips

Cover slips were chemically activated to allow stable, covalent formation of polyacrylamide sheets according to the protocol of Pelham and Wang[44], with modifications[69]. Briefly, a glass cover

slip (No. 1, 15 mm diameter; Fisher Scientific, Pittsburgh, PA) was coated with a small drop of 3-aminopropyltrimethoxysilane (TESPA, Sigma, St. Louis, MO), which was spread evenly on the surface. After 5 minutes, the coverslips were washed extensively with distilled water and then were autoclaved (121ºC at 1.5 atm) for 1 hour. The coverslips were transferred, treated side up, into plastic petri dishes and covered with 0.5% glutaraldehyde in phosphate buffered saline (PBS) (prepared by diluting 1 part of 70% stock solution, Polysciences, Inc., Warrington, PA, with 140 parts of PBS). After incubation at room temperature for 30 minutes, the coverslips were washed 5 times in distilled water on a shaker, for 10 minutes per wash, and allowed to dry in air. The treated coverslips were stored in a petri dish for up to 48 hours after preparation.

Creation of Polyacrylamide Gels

Thin sheets of polyacrylamide gel were prepared and bonded to the activated glass surface of the cover slips according to Pelham and Wang with modifications by Janmey[44]. Acrylamide (Bio-Rad, Hercules, CA, 30% w/v) was mixed with N, N-methylene-bis-acrylamide (BIS, Bio-Rad, 2.5% w/v) and distilled water to obtain a

final concentration of 10% acrylamide and 0.03% bisacrylamide. For more rigid or more flexible substrata the percentage of bisacrylamide was increased or decreased according to a previously established nonogram[44]. After the acrylamide/bisacrylamide solution was combined, polymerization was initiated by addition of ammonium persulfate (10% w/v solution, Bio-Rad, 1:200 volume) and N,N,N,N-tetramethyl ethylenediamine (TEMED, Bio-Rad, 1:2000 volume). Twenty-five microliters of the acrylamide solution was immediately placed onto the surface of an activated coverslip and the droplet was flattened using a large circular cover slip (No. 1, 22 mm diam., Fisher Scientific) covered in Sigma-Cote (SL-2 100ml, Sigma-Aldrich). After polymerization for 30 minutes, the circular cover slip was removed and the gels were agitated on a shaker in 500 µl HEPES (50 mM, pH 8.5) and then transferred to a 24 well plate. The HEPES was removed from the wells and a solution of 40 µl of Sulfo-SANPAH (0.5mg in 1ml of distilled water, Pierce Chemicals, Rockford, IL) was applied to each gel. The surface of each gel was then exposed to UV light from a 30 W germicidal lamp for 10 minutes. The glass-supported polyacrylamide sheets then underwent three washes of

500 µl HEPES (50mM, pH 8.5). The polyacrylamide sheets were then covered with a 200 µl solution of laminin (1mg/ml natural mouse laminin in 5.95ml HEPES buffer, Invitrogen™) and were incubated at 37ºC for 4 hours in 5% CO_2. The gels were then washed three times with 500 µl of PBS to prepare the polyacrylamide coated cover slips for cell culture. The gels were immersed in 500 µl of retinal pigment epithelium media (225ml Dulbucco's modified Eagle medium, 25ml of fetal bovine serum, and 1% penicillin streptomycin) 15 minutes prior to applying ARPE-19 cells at 20,000 (cells/ ml) per gel. Substrates of 500 Pa, 1000 Pa, 5000 Pa, and laminin-coated glass were created for this study.

Cell Culture

ARPE-19 cells were grown on the gels at 37ºC for 14 days in 5% CO_2, in 500 µl of retinal pigment epithelium media and the media was changed every other day. After 14 days in culture, 35 µl of bead solution (20 µl latex fluorescent beads (Polysciences Inc., diameter 1.967µm) suspended in 4ml of PBS) were added to each well, and incubated at 37ºC for 4 hours in 5% CO_2.

Flow Cytometry

After a 4-hour incubation period, all media were removed and the gels were washed three times with 500 µl of PBS. Trypsin-EDTA (200 µl of 0.05%) was added to each well and the gels were incubated at 37ºC for 15 minutes in 5% CO_2. The cells were then collected into separate, sterile, 15ml conical tubes. Each tube was centrifuged for 8 minutes at 800 RPM, at room temperature. Excess media was removed from the conical tubes and the cells were resuspended in 3 ml of PBS and 350 µl of the resulting solution was transferred to flow cytometry tubes for processing. Retinal pigment epithelium suspensions were analyzed in a flow cytometer (BD FACSCanto II, BD Biosciences) to obtain the number of cells with phagocytosed beads. The DAPI signal intensity obtained from the beads allowed quantification of the number of cells that phagocytosed a fluorescent bead.

Data Analysis

The number of cells that phagocytosed a bead was corrected for the total number of events analyzed. Linear regression was performed to evaluate the dependence of retinal pigment epithelium cell

phagocytosis on varying substrate stiffness. The forward scatter channel (FSC) and side scatter channel (SSC) were gated to select viable cells and avoid cellular debris[74]. Negative controls in which latex beads were not added to ARPE-19 cells were also included.

Results

ARPE-19 cells demonstrated an inverse linear relationship between substrate elastic modulus and phagocytosis (Figure 1). ARPE-19 cells cultured on the highest elastic modulus, laminin-coated glass, exhibited the least amount of phagocytosis.

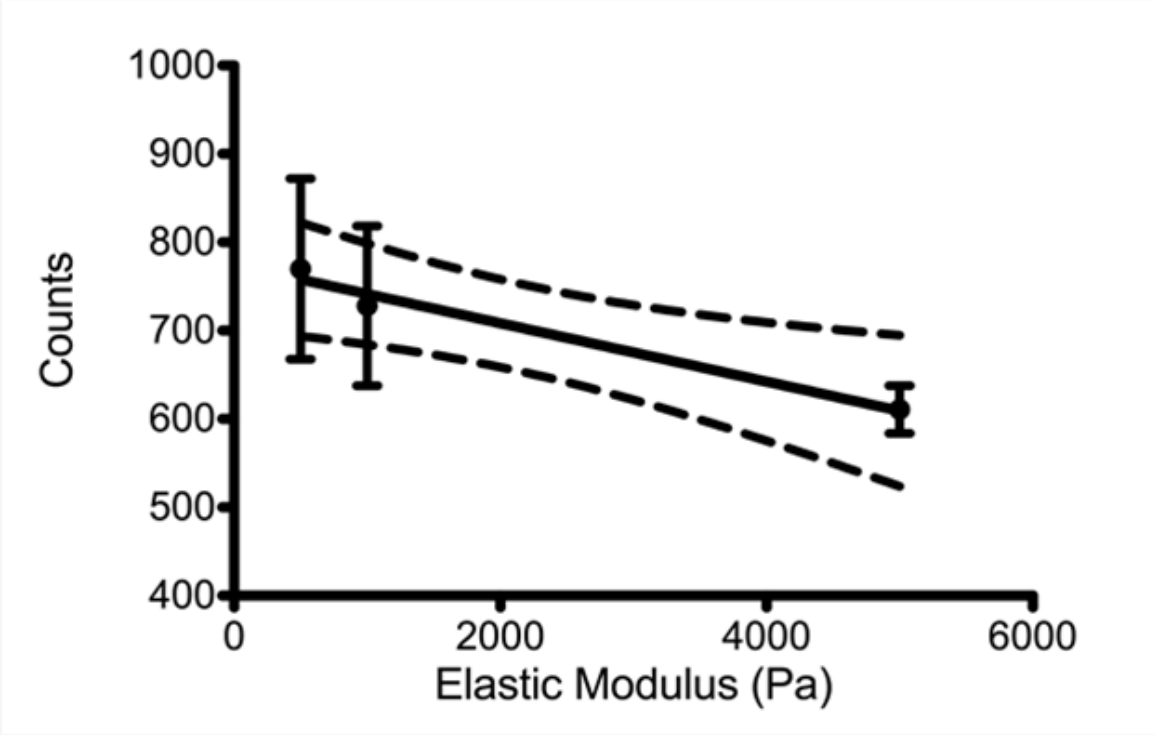

Figure 3.1: The mean and standard error of the mean plotted with the results of a linear regression analysis. The dashed lines indicate 95% confidence intervals; p=0.0135.

Discussion

Decreased phagocytosis by ARPE-19 cells cultured on substrates of higher elastic moduli suggests that changes in the stiffness of Bruch's membrane may affect retinal pigment epithelial cells *in vivo*. As Bruch's membrane ages, retinal pigment epithelial cells may be less able to phagocytose the outer segments of photoreceptor cells, and this may eventually lead to the accumulation of drusen on Bruch's membrane. In turn, retinal pigment epithelium dysfunction may affect photoreceptor function, causing the loss of central vision in the macula.

The results obtained in this experiment demonstrate that ARPE-19 cell phagocytosis is influenced by the stiffness of the cellular environment. Therefore, decreased phagocytosis by retinal pigment epithelial cells on higher elastic moduli could possibly play a role in the development of dry macular degeneration in older adults.

A weakness of this study is the use of a cell line, rather than primary retinal pigment epithelial cells. But, it is known that, in a variety of cell types including retinal Müller cells[69], kidney epithelial cells[44], and

numerous cellular processes, including cell spreading and motility[36] are influenced by substrate elastic modulus.

Possible areas for further investigation include a study of the rate of phagocytosis of retinal pigment epithelial cells grown on substrates of different elastic moduli, performed by leaving the beads in culture for different time intervals. Testing a wider range of substrate elastic moduli might provide more data and additional insight into this phenomenon.

Currently, there is substantial interest in developing synthetic substitutes for Bruch's membrane for the culture of retinal pigment epithelial cells, for eventual transplantation into patients suffering from macular degeneration. Our study suggests that the elastic modulus of these substrates may be a critical design parameter.

CONCLUSION

As was stated in the beginning of this dissertation, the theory of the mechanical environment influencing the phenotypic and genetic fate of cells was first established in the 1980s. Over time, this idea became slowly accepted, particularly following the work of Adam Engler and Dennis Discher[38] in which adult meschymal stem cells were induced to differentiate into different fates (neurons, muscle, and bone) by only changing substrate stiffness. What this dissertation has been undertaken to study, is that specific problems and diseases that exist in the retina can be influenced by the changing mechanical environment. These problems may also be alleviated by limiting those changes to the environment. While scar formation is a definite hindrance to the regrowth of neuronal tissue, it is without doubt a necessary evil. Creations of biocompatible and penetrable hydrogels to use as vitreous substitutes can suppress this glitotic activity by filling in cavities left by the dead cells so that neurons can reform. This would reduce the occurrence of proliferative vitreoretinopathy and thereby limit the number of surgeries that are undertaken to repair trauma to the retina. These gels can have further impact on

stroke victims and other central nervous system trauma. The discovery of changes in the Yes-associated protein/taffazin complex has only served to show how much more can possibly be learned about how the cytoskeleton sends information to the nucleus. Specifically, how the tension in extracellular matrix gets transmitted to the cytoskeleton and then to influence transcription factors is still under study. Better understanding of these signal transduction pathways in specific cells, particularly cells as involved in regeneration, as Müller cells are, potentially increases the abilities of regenerative therapies to properly treat related diseases.

While my research on cellular reaction to the underlying substrate can be problems of retinal diseases and trauma, retinal prosthetics and retinal regeneration, an increasing area of technology to combat blindness[75, 76], may benefit from this research. The materials currently being used in these applications tend to be markedly different in mechanical properties from the cellular environment. Materials such as metal pins, silicon sheets, and carbon nanotubes are all detrimental to the normal functioning of cells[34, 35, 77]. My research seeks to better integrate devices into the body to help

increase functionality, by reducing the amount of scar tissue that will form around the device, which will allow the neurons better device contact and to be better stimulated by impulses from the device. Finding new and better ways to prevent metaplasia, but also to prevent apoptosis of cells that are either implanted or simply exposed to the after effects of trauma, will increase our abilities to treat many diseases and injuries as well as having the potential to limit the occurrence of disabilities. This line of research has the ability to change the world of medicine.

APPENDIX

Preparing Gels

Preparing 15mm coverslips to be coated with gels and eventually plate cells on is not easy and took some time to optimize (especially with large hands). To start with, I did away with the sodium hydroxide wash that was stated in the Yang and Mills paper. Most of the time it just ended up making the coverslips cloudy with a film that would hinder the 3-aminopropyltrimethsiloxilane (TESPA) from binding properly, and with the extra autoclave step a prior sterilization wash seemed somewhat redundant. When adding the TESPA to the glass, it is best to use the smallest drop you can get to come out and then spread that around with your finger, making sure you cover the entire surface. After this has been allowed to dry, it should be washed with a squirt bottle which will cause the excess TESPA to crack and eventually fall off. This is to be expected; only a very thin film is needed to be effective. If too much of the excess is left on the glass, when they are wrapped in foil with paper interleaved between, the paper will stick to the glass. The hydrophobic preparation of the coverslips is much easier. Since it is extremely volatile, large drops

can be used to treat several coverslips at a time and the excess will evaporate. Also, after the hydrophobic coverslips have been autoclaved they are reusable if they are kept sterile. I have found it best to place all the foil packets (TESPA-coated, Sigmacote-treated, and untreated) into a glass beaker with two sets of forceps and a large piece of foil, and then seal the top of the beaker. Once the autoclave has been performed, let the beaker cool down before it is transferred into the tissue culture hood.

In the hood, use the sterile forceps to move everything. The TESPA treated coverslips are removed first and placed in a petri dish, each dish can hold around 12-15 coverslips depending on spacing. Once they are in the petri dish, you can pour on the gluteraldehyde solution for 30 minutes. The solution should be premixed in a conical tube, and is best to use 14 mL of PBS mixed with 100 µL of 70% gluteraldehyde per petri dish. After the incubation, the solution and subsequent three washes of di-water need to be placed into hazardous waste. Leave the water of the last wash in the petri dish, if you do not the surface tension of the thin layer of water that will be left makes it very difficult to lift the coverslips off the bottom. The large

piece of foil should be spread out in the hood for the coverslips to be placed on while they dry.

The coverslips need to be completely dry, top and bottom, before the polyacrylamide is added. If not, the captured water left underneath the coverslip could lead to the gel being pulled under the coverslip by capillary action and there is enough trouble with that happening when dry if the top coverslip slides around too much. After the polyacrylamide mixture is prepared, it must be filtered. So must the TEMED and ammonium persulfate, which should be filtered separately to ensure the gel does not set before it is placed on the coverslip. When ammonium persulfate and TEMED are added, immediately pipette the acrylamide on to the coverslips and cover with the Sigmacote-treated coverslip and watch the spread so that as much of the coverslip is covered as possible. If necessary, the top coverslip can be pressed down or slowly slid around to help spread the liquid. When the gel that is left in the tube has set, you can be sure the gel on the coverslips is set as well. The top coverslips can be removed and set aside in a clean petri dish to be reused for the next round. The gel coated slips should be placed immediately into

the 24-well plate and covered with HEPES buffer, which will count as the wash for the Sulfo-SANPAH, still moving everything with forceps of course. The 24-well plate can then be placed in the refrigerator until the cells are ready to be plated. As long as the gels remain hydrated, the laminin does not need to be placed on immediately but once the laminin is on the gel the cells need to be plated within 24 hours.

Laminin Procedures

Everything should be thawed before beginning. Laminin must be removed from the -80^{o}C freezer and placed on ice to thaw slowly so that it does not bind together. Sulfo-SANPAH is quite moisture sensitive and thus if it is not at room temperature before opening condensation can form inside the bottle, causing it to clump. When things are ready the lights should be turned as low as possible to avoid activating the Sulfo-SANPAH before it is on the gel. Approximately one-half of a milligram should be weighed out into a microcentrifuge tube and should be suspended in one milliliter of DI water. Small volumes (around 40-50 microliters for a 24-well plate) should be placed in each well and allowed to cover the gel, then

immediately placed 6 inches from a UV light for around 8 minutes, or until it darkens. Once done with the UV you can wash 3 times with HEPES buffer. While you are doing this, prepare your Laminin solution. The 50 microliter aliquot will be mixed with 4.95 mL of HEPES and mixed thoroughly (the 5 mL solution should be just enough for all 24-wells). Place 200 µL in each well and make sure the slides stay SUBMERGED (they will try to float in the beginning), immediately incubate for 4 hours at 37^{o}C. After the 4 hours is done, remove liquid and apply a working volume of cell media for at least 15 minutes before cells are plated, must plate cells within 24 hours.

Extracting and Plating Cells

To remove cells from culture in a petri dish you must first collect 15mL conical tubes for each dish or a 50mL for every 3 dishes, also thaw and warm the 0.5% or 5% Trypsin (depending on Muller or RPE cells respectively), PBS, and fresh media in the water bath. The old media that is on the cells before you begin should be set aside into the tube. Next, wash the dish with 5 mL of PBS to ensure complete removal of the old media and its excess proteins which would keep the Trypsin for degrading the attachment proteins of the cells. Add 3

mL of Trypsin to the dish and place in the incubator (2 minutes for Müller cells, 5-10 minutes for RPE) the cells can be checked for detachment with the inverted microscope. When the incubation is done, pour the old media from the tube into the dish. This will stop the trypsin from continuing to degrade the cellular proteins. The trypsin/media mixture should be pipetted back into the centrifuge tube and spun down (800 rpm for 5 minutes). The separated solution can be pipetted off leaving the solid pellet, which should be re-suspended in fresh media before being plated in new dishes.

PCR

A polymerase chain reaction (PCR) is a test which involves removing the mRNA from cells and, through reverse transcription, creating cDNA copies of the transcribed genes. Once the cDNA has been created, the PCR will exponentially increase the DNA yield so that the fluorescent signal can be read.

Since it does involve extracting RNA, gloves must be used at all times. RNAse, the enzyme which breaks down RNA, is present on human skin so the gloves help protect the transfer to anything used.

You also must watch anything that you touch with the gloves on, because if someone touched the same object earlier without gloves then it could transfer RNAse to your gloves. If you feel that there is any possibility your gloves have been contaminated, immediately replace with a new pair.

Remove the cells from the wells and place them in a centrifuge tube from a newly opened bag. Pellet the cells as usual and resuspend in 150 µl of RNAse free PBS (do not use more than 10^7 cells in the RNA extraction). Centrifuge at 300g for 5 mins before aspirating supernatant.

Isolate the mRNA using Quiagen RNeasy Mini Kit starting by flicking the pellet to loosen then adding between 350-600µl of buffer RLT (depending on cell count).

Vortex or pipette to mix.

Pass the lysate at least 5 times through a blunt 20-gauge needle attached to an RNAse free syringe (DO NOT GENERATE BUBBLES).

Add enough 70% ethanol to make 700µl in total

Transfer all, including any precipitate that may have formed, to an RNeasy spin column placed in a 2ml collection tube. (DO NOT TOUCH THE RESIN ON THE INSIDE OF THE COLUMN OR TUBE WITH YOUR PIPETTE TIP).

Close the lid gently and centrifuge at >10,000 rpm for 15s

Discard the liquid in the collection tube but reuse the tube itself. Be careful that the spin column does not come into contact with the flow through and empty the collection tube completely. Do not set the spin column on the counter, either hold it by the top in your hand until the collection tube is clean and it can be replaced, or put into a brand new 1.5 ml tube to hold. Do not mix spin columns with other collection tubes.

Add 700ml of buffer RW1 to the spin column

Close lid gently and centrifuge at >10,000 rpm for 15s

Discard the liquid in the collection tube but reuse the tube itself.

Buffer RPE is supplied as a concentrate. Make sure Ethanol has been added to the buffer before use.

Add 500 µl of buffer RPE to the spin column

Once again centrifuge at >10,000 rpm for 15s

Discard flow through

Add 500 µl of buffer RPE

Centrifuge for 2 mins at >10,000 rpm to wash spin column membrane.

Discard the spin column with the flow through, and place the spin column in a new 2ml collection tube

Close lid and spin for 1 min at full speed without adding any liquid, to make sure all liquid has been removed.

Place RNeasy spin column in a new 1.5 ml tube. Add 30-50µl of RNAse free water directly to the spin column.

Centrifuge for 1 min at >10,000 rpm to elute RNA

Remove 5 µl of the liquid into a new tube for analysis and keep on ice. The rest should be placed at -80^{o}C until experiments are set.

To analyze the mRNA, you must first use a Nanodrop spectrophotometer to find out how many ng/µl you have. Then use

the Agilent RNA Nano chip (which holds 12 samples) to analyze the quality of the RNA (low quality means it has been degraded by RNase)

The concentration of RNA is to be determined by measuring the absorbance at 260 nm in the spectrophotometer

To ensure significance, readings should be between 0.15 and 1.0

An absorbance of 1 unit at 260 nm corresponds to 40 µg or RNA per ml

The ratio of the readings at 260 nm and 280 nm (A260/A280) provides an estimate of the purity of RNA with respect to contaminants that absorb in the UV, such as protein.

Preparing Nano chip

Warm components of RNA nano kit to room temperature for 30 minutes

Pipette 550µl of RNA 6000 Nano gel matrix (red) into spin filter.

Centrifuge at 1500g for 10 minutes at room temperature

Aliquot 65µl filtered gel into 0.5ml RNase-free microfuge tubes. Use filtered gel within 4 weeks.

Allow the RNA 6000 Nano dye concentrate (blue) to equilibrate to room temperature for 30 min

Vortex RNA 6000 Nano dye concentrate (blue) for 10 seconds, spin down, and add 1µl of dye into a 65µl aliquot of filtered gel.

Vortex solution well, spin tube at 13000g for 10 minutes at room temperature. Use prepared gel-dye mix within one day

Dilute samples with elution buffer to the concentration recommended in the Agilent RNA kit manual. Aim for the middle of the range whenever possible.

Denature your RNA samples (and the ladder if it is the first time that the ladder has been used) BE SURE TO DENATURE before you start setting up the chip and hold the samples at 4C until ready to load the chip.

Practice “reverse pipetting” before you start loading the gel chip (reverse pipetting is pushing the plunger past the stopping point when

taking in to the pipette, and only pushing the plunger to the stopping point when expelling and should be used at all times when loading the chip)

Put a new RNA 6000 Nano chip on the chip priming station.

Check that the plunger clip is in the right position.

Pipette 9.0µl of gel-dye mix in the well marked with a “G”

Make sure that the plunger is positioned at 1ml and then close the chip priming station.

Press plunger until it is help by the clip.

Wait exactly 30s then release clip.

Wait for 5s. Slowly pull back the plunger to the 1ml position.

Open chip priming station and pipette 9.0µl of gel-dye mix in the wells marked.

Discard the remaining gel-dye mix.

Pipette 5µl of RNA 6000 Nano marker (green) in all 12 sample wells and in the well marked with a picture of a ladder.

Pipette 1µl of prepared ladder in well marked with a ladder

Pipette 1µl of sample in each of the 12 sample wells. Pipette 1µl of RNA 6000 Nano Marker (green dot) in each unused sample well.

Put the chip horizontally in the adapter of the IKA vortexer and vortex for 1min at 2400rpm.

Run the chip in the Agilent 2100 bioanalyzer within 5 mins.

Western Blot

In the Western blot protocol, PBST refers to PBS with 5% Tween-20

1) Set microcentrifuge temp to 4^{o}C. Get bucket of ice. Turn on heat block.

2) Prepare 500 ml 1X home-made running buffer. 50ml 10X running buffer + 450ml Milli H_2O. Place running buffer at 4^{o}C

3) Check pH of all solutions, and adjust if necessary:

    a) 1.5M Tris for resolving gel (at 4oC): 8.8

    b) Stacking gel buffer: 6.8

c) Running buffer: 8.3

4) Prepare 10ml 9.95% resolving gel:

a) 5.1ml Milli water

b) 2.3ml 40% acrylamide/bis 37.5:1

c) 2.5ml 1.5M Tris pH 8.8 (at 4^{o}C)

d) 100µl SDS

e) De-gas above solution for 15 min

f) Add 50µl 10% ammonium persulfate (fresh), and 10µl TEMED. Use transfer pipette to mix solution without mixing air

g) Pour gels quickly and overly slowly with RO water, being careful to make an even interface.

5) Cover with plastic wrap and sat at least 1hr at room temp.

6) Prepare stacking gel: (use comb)

a) 2.625ml stacking gel buffer pH 6.8

b) 0.45ml 40% acrylamide/bis 37.5:1

c) 60µl 10% APS (fresh)

d) 5.5µl TEMED

e) Pour stacking gel and be zealous about removing all bubbles

f) Allow gel to set for at least 45 mins

7) Prepare protein samples

a) Prepare 1 ladder sample with the protein samples. Thaw, but keep on ice

b) Vortex, then spin down insolubles at 4^{o}C

c) 950µl Laemmli buffer must be mixed with 50µl β-mercaptoethanol

d) Prepare protein samples accordingly: Dilute protein sample with equal parts Bio-Rad Laemmli buffer

8) Do SDS-PAGE:

a) Vortex and spin protein samples. Boil samples and 100µl ladder at 99^{o}C 10 min using lid clamps.

b) Set up electrophoresis apparatus using cold running buffer. Eliminate bubbles. Flush wells with running buffer.

c) Load protein samples: 20-30µl protein, 5-10µl ladder depending on well size.

d) Run at 200V (constant voltage) for 45 mins or until ladder has extended to bottom of gel.

9) Make transfer buffer while gel is running

a) 3.2g Tris Base

b) 14.4g UltraPure glycine

c) 200ml Methanol

d) Deionized water to 1L final volume

10) Transfer Procedure:

a) Cut nitrocellulose and 3MM filter paper slightly larger than the gel. Mark nitrocellulose in upper corner with antibody type.

b) Fill 1 tray with Milli-Q water and 4 trays with transfer buffer.

c) Trim stacking gel off and cut bottom corner of resolving gel on side nearest ladder to help future orientation.

d) Turn gel over and float gel off into transfer buffer. Allow gel to equilibrate 15min-1hr.

e) Prepare gel sandwiches (keep all components submerged)

   i) Place a scrubby pad on black plate.

   ii) Capture the gel on top of filter paper: cut corner is up and on opposite side of original orientation. Place paper and gel on scrubby pad.

   iii) Place the nitrocellulose membrane on top of the gel, marked side facing gel.

   iv) Place the second sheet of filter paper on top of the membrane, then second scrubby pad.

   v) Press down gently in the center and smooth out to the sides to remove bubbles.

f) Place cassette in module. Add the frozen Bio-ice cooling unit.

g) Fill tank completely with transfer buffer. Add a small stir bar and place on a stir plate.

h) Run at 40 V for 120 min

i) Check and readjust pH of PBS, PBST, and 4% non-fat milk in PBST: pH 7.6

11) Blocking:

a) Disassemble cassettes and make sure ladder is completely transferred from the gel to the membrane. Peel off the nitrocellulose membranes.

b) Rinse membrane with PBS for 5 min with rotation at room temp.

c) Transfer membranes to trays containing about 25ml 2% milk in PBST

d) Block 1 hr

12) Primary Antibody:

a) Make antibody dilutions with 2% Milk in PBST

b) Pour off blocking solution and pipette on antibody.

c) Turn membranes protein-side down. Wrap trays in plastic, and place on rotator with vigorous rotation at room temp for 1hr

d) Incubate overnight at 4^{o}C

Day 2: Protein Imaging

1) Remove membranes from 4^{o}C and rotate at room temp 1hr
2) Make secondary antibody with 2% milk in PBST
3) Remove primary antibody and save. Flip membranes protein-side up
4) Wash 3 times in PBST for 5 minutes each
5) Wash 3 times in PBS for 5 minutes each
6) Wash with blocking buffer 5 minutes
7) Pour on secondary antibody, flip membrane protein-side down
8) Incubate at room temp with rotation for 1 hr. Take out ECL kit to bring to room temp
9) Remove secondary antibody, flip protein-side up

10) Wash 3 times PBST 5 min then 4 times PBS 5 min. Turn on film developer during PBS washes

11) Luminol+H_2O_2 1:1, pour on membrane to cover evenly, treat 1 min. Sandwich between plastic sheets and roll out bubbles.

12) Image first with camera, then with film.

13) Rinse with PBS (5 min on rotator)

14) Place in blocking buffer overnight at 4^{o}C

Day 3: Control Protein

1) Make GAPDH primary antibody:

2) Remove membrane from 4^{o}C. Pour off blocker, pour on primary antibody. Flip membrane protein side down.

3) Rotate at room temp 2 hrs

4) Make secondary antibody

5) Remove primary antibody and save. Flip membrane protein-side up

6) Wash 5 minutes each with rotation at room temp: 3x PBST, 3x PBS, 1x blocking buffer

7) Pour on secondary antibody, flip membrane protein-side down

8) Incubate at room temp with rotation for 1hr. Take out ECL kit and bring to room temp

9) Remove secondary antibody, flip membrane protein side up.

10) Wash 5 min with rotation at room temp: 3x PBST, 4x PBS. Turn on film developer during PBS washes

11) Luminol+H_2O_2 1:1, pour on membrane to cover evenly, treat 1 min. Sandwich between plastic sheets and roll out bubbles.

12) Image first with camera, then with film

Set membranes on filter paper to dry. Fill out card with all necessary information. When membranes dry, sandwich between plastic wrap and tape to blot card.

Immunohistochemistry

Immunohistochemistry is simply the staining of fixed cells for proteins which you are interested in. In general, the antibodies used for this are relatively large and as such are unable to pass through the cell membrane. It is for this reason that the cells are fixed (soaked in paraformaldehyde so that they are dead but the protein structure remains locked in place). After they are fixed the membrane can be permeabilized with washes so that the antibodies can flow through.

1. Using clean forceps, transfer coverslip with gel to clean culture dish (gel side up) (not possible in the 24-well plate)
2. Wash gently 3x PBS, 15 min each (use large volumes
3. Fix 4% PFA in phosphate buffer 25 min room temp
4. Wash 4x PBS (use large volumes-make sure gel is well covered) 10 min each rotator, low speed (to get PFA out of gel)
5. Block (blocking buffer) at least 4 hours room temp on rotator at low speed (200µl per well in 24 well plate)
6. Prepare antibodies according to pre-determined concentrations in blocking buffer

7. Pipette on primary antibodies and incubate for 1 hour at room temp with rotation at low speed; followed by overnight at 4C (no rotation but sealed to prevent evaporation)
8. Remove antibodies and reserve (can be stored and tested for reuse if 0.01% sodium azide is added as preservative)
9. Wash 3x PBS + 0.5% TritonX100 for 15 minutes
10. Dilute secondary antibody in blocking buffer
11. Cover with foil to protect secondary antibodies from light
12. Add enough to cover gel
13. Incubate 4 hours room temp with rotation at low speed
14. Wash 3x PBS + 0.5% TritonX100 15 min each
15. Counterstain with PBS containing 1:5000 Hoechst 33342 (Blue nuclear stain)
16. Wash PBS 3 x 15 min
17. Photograph

Blocking buffer:

10% Normal goat serum

5% BSA

0.5% TritonX100

1% Fish Gelatin

Diluted in PBS

ELISA

The purpose of enzyme-linked immunosorbant assay (ELISA) is to make succeeding layers of protein, the topmost of which is labeled with a marker which will cause the liquid to change color. This color change can be read by a spectrophotometer which will measure how much the light of a certain wavelength was absorbed. The steps for which are:

1. Prepare all reagents, working standards, and samples properly
    a. Protein samples should be diluted to within the working range of the assay
    b. All reagents should be brought to room temperature for 30 minutes before starting
        i. Anitbodies require a 100:1 dilution
        ii. Wash buffer uses a 25:1 dilution

c. Standards must be diluted serially so that each successive well has half the concentration of the proceeding

2. Add 100µl of standard or sample per well and cover with an adhesive strip
3. Incubate for 2 hours at 37^{o}C
4. Remove the liquid from each well but DO NOT WASH
5. Add 100µl of diluted Biotin-antibody to each well. Cover with a fresh adhesive strip (if diluted antibody appears cloudy pipette to mix at room temperature)
6. Incubate for 1 hour at 37^{o}C
7. Aspirate each well and wash 3 times. Wash by filling each well with wash buffer using a squirt bottle or multi-channel pipette. Let stand for 2 minutes then completely remove all liquid (complete removal of liquid is essential at each step). Remove by decanting and then patting against absorbent paper.
8. Add 100µl of diluted HRP-Avidin. Cover with a fresh adhesive strip.
9. Incubate for 1 hour at 37C

10. Aspirate each well and then wash 5 times as in step 8
11. Add 90µl of TMB substrate to each well.
12. Incubate 15-30 minutes at 37C (time is dependent on concentration, remove from incubation before the color of any well gets too deep). Protect from light.
13. Add 50µl of stop solution to each well
14. Gently tap the plate to ensure thorough mixture
15. Determine optical density of each well within 5 minutes using a microplate reader at 450 nm. Standards can be used to create a linear fit of optical density vs protein concentration to give accurate concentrations for each well.

Glass vs Plastic

When investigating protein expression using Western blot, I tried to grow cells on tissue culture plastic instead of a glass coverslip with no gel. This was undertaken with the assumption that the elastic modulus for plastic, while not the same, was near enough to glass that any differences in expression would be minute. I also chose this course to save time as preparing the glass coverslips can be aggravating. What happened was a large increase in Tenascin-C

expression on plastic as opposed to glass. What was also seen, when looking at the total protein for normalization purposes, was a distinctly different banding from the cells grown on the plastic substrate versus those grown on the glass or even the gels (Figure A.1). While it is not currently known why this is, whether it is a whetting property of the plastic as opposed to glass or a treatment of the plastic causing different binding properties, it should be noted to be a factor. DO NOT USE TISSUE CULTURE PLASTIC AS AN ANALOG FOR GLASS.

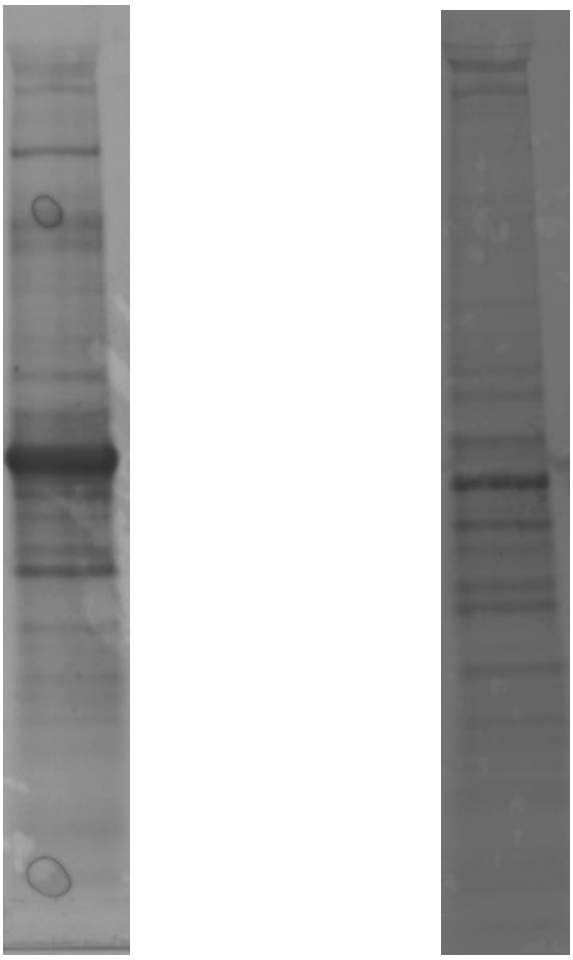

Figure A.1: The total protein expression of cells grown on glass (left) and tissue culture plastic (right). Notice the distinctly different banding patterns, particularly around the middle range (possibly Vimentin).

BIBLIOGRAPHY

1. Leaver, P.K., *Proliferative vitreoretinopathy.* Br J Ophthalmol, 1995. **79**(10): p. 871-2.
2. Casaroli-Marano, R.P., R. Pagan, and S. Vilaro, *Epithelial-mesenchymal transition in proliferative vitreoretinopathy: intermediate filament protein expression in retinal pigment epithelial cells.* Invest Ophthalmol Vis Sci, 1999. **40**(9): p. 2062-72.
3. Pekny, M., et al., *The impact of genetic removal of GFAP and/or vimentin on glutamine levels and transport of glucose and ascorbate in astrocytes.* Neurochem Res, 1999. **24**(11): p. 1357-62.
4. Baumann, N. and D. Pham-Dinh, *Biology of oligodendrocyte and myelin in the mammalian central nervous system.* Physiol Rev, 2001. **81**(2): p. 871-927.
5. Jessen, K.R. and R. Mirsky, *Glial cells in the enteric nervous system contain glial fibrillary acidic protein.* Nature, 1980. **286**(5774): p. 736-737.

6. Azevedo, F.A., et al., *Equal numbers of neuronal and nonneuronal cells make the human brain an isometrically scaled-up primate brain.* J Comp Neurol, 2009. **513**(5): p. 532-41.

7. Stichel, C.C. and H.W. Muller, *The CNS lesion scar: new vistas on an old regeneration barrier.* Cell Tissue Res, 1998. **294**(1): p. 1-9.

8. Faulkner, J.R., et al., *Reactive astrocytes protect tissue and preserve function after spinal cord injury.* J Neurosci, 2004. **24**(9): p. 2143-55.

9. Sarthy, P.V. and D.M. Lam, *Biochemical studies of isolated glial (Muller) cells from the turtle retina.* J Cell Biol, 1978. **78**(3): p. 675-84.

10. Linser, P. and A.A. Moscona, *Induction of glutamine synthetase in embryonic neural retina: localization in Muller fibers and dependence on cell interactions.* Proc Natl Acad Sci U S A, 1979. **76**(12): p. 6476-80.

11. Liaw, S.H., I. Kuo, and D. Eisenberg, *Discovery of the ammonium substrate site on glutamine synthetase, a third cation binding site.* Protein Sci, 1995. **4**(11): p. 2358-65.

12. Suarez, I., G. Bodega, and B. Fernandez, *Glutamine synthetase in brain: effect of ammonia.* Neurochem Int, 2002. **41**(2-3): p. 123-42.

13. Franze, K., et al., *Muller cells are living optical fibers in the vertebrate retina.* Proc Natl Acad Sci U S A, 2007. **104**(20): p. 8287-92.

14. Bhattacharjee, J. and S. Sanyal, *Developmental origin and early differentiation of retinal Muller cells in mice.* J Anat, 1975. **120**(Pt 2): p. 367-72.

15. Meller, K. and W. Tetzlaff, *Scanning electron microscopic studies on the development of the chick retina.* Cell Tissue Res, 1976. **170**(2): p. 145-59.

16. Phillips, J.B., et al., *Harmonin (Ush1c) is required in zebrafish Muller glial cells for photoreceptor synaptic development and function.* Dis Model Mech, 2011. **4**(6): p. 786-800.

17. Johns, P.R. and S.S. Easter, Jr., *Growth of the adult goldfish eye. II. Increase in retinal cell number.* J Comp Neurol, 1977. **176**(3): p. 331-41.

18. Otteson, D.C. and P.F. Hitchcock, *Stem cells in the teleost retina: persistent neurogenesis and injury-induced regeneration.* Vision Res, 2003. **43**(8): p. 927-36.

19. Yurco, P. and D.A. Cameron, *Responses of Muller glia to retinal injury in adult zebrafish.* Vision Res, 2005. **45**(8): p. 991-1002.

20. Thummel, R., et al., *Inhibition of Muller glial cell division blocks regeneration of the light-damaged zebrafish retina.* Dev Neurobiol, 2008. **68**(3): p. 392-408.

21. Bernardos, R.L., et al., *Late-stage neuronal progenitors in the retina are radial Muller glia that function as retinal stem cells.* J Neurosci, 2007. **27**(26): p. 7028-40.

22. Trappmann, B., et al., *Extracellular-matrix tethering regulates stem-cell fate.* Nat Mater, 2012. **11**(7): p. 642-9.

23. Khetan, S. and J.A. Burdick, *Patterning network structure to spatially control cellular remodeling and stem cell fate within 3-dimensional hydrogels.* Biomaterials, 2010. **31**(32): p. 8228-34.

24. Qiu, Y. and K. Park, *Environment-sensitive hydrogels for drug delivery.* Adv Drug Deliv Rev, 2001. **53**(3): p. 321-39.

25. Dimitriadis, E.K., et al., *Determination of elastic moduli of thin layers of soft material using the atomic force microscope.* Biophys J, 2002. **82**(5): p. 2798-810.

26. Kumar, V., et al., *Robbins and Cotran pathologic basis of disease*. 7th ed. 2005, Philadelphia: Elsevier Saunders. xv, 1525 p.

27. Alberts, B., *Essential cell biology*. 2nd ed. 2004, New York, NY: Garland Science Pub. xxi, 740, 102 p.

28. Alberts, B., *Essential cell biology*. 3rd ed. 2009, New York: Garland Science.

29. Footer, M.J., et al., *Direct measurement of force generation by actin filament polymerization using an optical trap.* Proc Natl Acad Sci U S A, 2007. **104**(7): p. 2181-6.

30. Pelham, R.J., Jr. and Y. Wang, *High resolution detection of mechanical forces exerted by locomoting fibroblasts on the substrate.* Mol Biol Cell, 1999. **10**(4): p. 935-45.

31. Caruthers, B., et al., *Surgical technology for the surgical technologist : a positive care approach*. 2001, Albany, NY: Delmar. xxi, 911 p.

32. Loudin, J.D., et al., *Optoelectronic retinal prosthesis: system design and performance.* J Neural Eng, 2007. **4**(1): p. S72-84.

33. Shoval, A., et al., *Carbon nanotube electrodes for effective interfacing with retinal tissue.* Front Neuroeng, 2009. **2**: p. 4.

34. Kolosnjaj, J., H. Szwarc, and F. Moussa, *Toxicity studies of carbon nanotubes.* Adv Exp Med Biol, 2007. **620**: p. 181-204.

35. Porter, A.E., et al., *Direct imaging of single-walled carbon nanotubes in cells.* Nat Nanotechnol, 2007. **2**(11): p. 713-7.

36. Georges, P.C. and P.A. Janmey, *Cell type-specific response to growth on soft materials.* J Appl Physiol, 2005. **98**(4): p. 1547-53.

37. Janmey, P.A., et al., *The hard life of soft cells.* Cell Motil Cytoskeleton, 2009. **66**(8): p. 597-605.

38. Engler, A.J., et al., *Matrix elasticity directs stem cell lineage specification.* Cell, 2006. **126**(4): p. 677-89.

39. Georges, P.C., et al., *Increased stiffness of the rat liver precedes matrix deposition: implications for fibrosis.* Am J Physiol Gastrointest Liver Physiol, 2007. **293**(6): p. G1147-54.

40. Lu, Y.B., et al., *Viscoelastic properties of individual glial cells and neurons in the CNS.* Proc Natl Acad Sci U S A, 2006. **103**(47): p. 17759-64.

41. Fisher, R.F., *The influence of age on some ocular basement membranes.* Eye (Lond), 1987. **1** (Pt 2): p. 184-9.

42. Otteson, D.C. and M.J. Phillips, *A conditional immortalized mouse muller glial cell line expressing glial and retinal stem cell genes.* Invest Ophthalmol Vis Sci, 2010. **51**(11): p. 5991-6000.

43. Pelham, R.J., Jr. and Y. Wang, *Cell locomotion and focal adhesions are regulated by substrate flexibility.* Proc Natl Acad Sci U S A, 1997. **94**(25): p. 13661-5.

44. Wang, Y.L. and R.J. Pelham, Jr., *Preparation of a flexible, porous polyacrylamide substrate for mechanical studies of cultured cells.* Methods Enzymol, 1998. **298**: p. 489-96.

45. Kerrison, J.B., et al., *Bone morphogenetic proteins promote neurite outgrowth in retinal ganglion cells.* Mol Vis, 2005. **11**: p. 208-15.

46. Byfield, F.J., et al., *Absence of filamin A prevents cells from responding to stiffness gradients on gels coated with collagen but not fibronectin.* Biophys J, 2009. **96**(12): p. 5095-102.

47. Yeung, T., et al., *Effects of substrate stiffness on cell morphology, cytoskeletal structure, and adhesion.* Cell Motil Cytoskeleton, 2005. **60**(1): p. 24-34.

48. Jat, P.S., et al., *Direct derivation of conditionally immortal cell lines from an H-2Kb-tsA58 transgenic mouse.* Proc Natl Acad Sci U S A, 1991. **88**(12): p. 5096-100.

49. Giannelli, S.G., et al., *Adult human Muller glia cells are a highly efficient source of rod photoreceptors.* Stem Cells, 2011. **29**(2): p. 344-56.

50. Guidry, C., *The role of Muller cells in fibrocontractive retinal disorders.* Prog Retin Eye Res, 2005. **24**(1): p. 75-86.

51. Rotsch, C., K. Jacobson, and M. Radmacher, *Dimensional and mechanical dynamics of active and stable edges in motile fibroblasts investigated by using atomic force microscopy.* Proc Natl Acad Sci U S A, 1999. **96**(3): p. 921-6.

52. Agrawal, N.J. and R. Radhakrishnan, *Calculation of free energies in fluid membranes subject to heterogeneous curvature fields.* Phys Rev E Stat Nonlin Soft Matter Phys, 2009. **80**(1 Pt 1): p. 011925.

53. Dertinger, S.K., et al., *Gradients of substrate-bound laminin orient axonal specification of neurons.* Proc Natl Acad Sci U S A, 2002. **99**(20): p. 12542-7.

54. Hinton, D.R., et al., *Novel growth factors involved in the pathogenesis of proliferative vitreoretinopathy.* Eye (Lond), 2002. **16**(4): p. 422-8.

55. Nagai, N., et al., *CTGF is increased in basal deposits and regulates matrix production through the ERK (p42/p44mapk) MAPK and the p38 MAPK signaling pathways.* Invest Ophthalmol Vis Sci, 2009. **50**(4): p. 1903-10.

56. He, S., et al., *Connective tissue growth factor as a mediator of intraocular fibrosis.* Invest Ophthalmol Vis Sci, 2008. **49**(9): p. 4078-88.

57. Kuiper, E.J., et al., *Connective tissue growth factor is necessary for retinal capillary basal lamina thickening in diabetic mice.* J Histochem Cytochem, 2008. **56**(8): p. 785-92.

58. Cui, J.Z., et al., *Stage specificity of novel growth factor expression during development of proliferative vitreoretinopathy.* Eye (Lond), 2007. **21**(2): p. 200-8.

59. Kita, T., et al., *Functional characteristics of connective tissue growth factor on vitreoretinal cells.* Diabetes, 2007. **56**(5): p. 1421-8.

60. Fuchshofer, R., et al., *Hypoxia/reoxygenation induces CTGF and PAI-1 in cultured human retinal pigment epithelium cells.* Exp Eye Res, 2009. **88**(5): p. 889-99.

61. Dupont, S., et al., *Role of YAP/TAZ in mechanotransduction.* Nature, 2011. **474**(7350): p. 179-83.

62. Provenzano, P.P., et al., *Matrix density-induced mechanoregulation of breast cell phenotype, signaling and gene expression through a FAK-ERK linkage.* Oncogene, 2009. **28**(49): p. 4326-43.

63. Sage, E.H. and P. Bornstein, *Extracellular proteins that modulate cell-matrix interactions. SPARC, tenascin, and thrombospondin.* J Biol Chem, 1991. **266**(23): p. 14831-4.

64. Chiquet-Ehrismann, R. and M. Chiquet, *Tenascins: regulation and putative functions during pathological stress.* J Pathol, 2003. **200**(4): p. 488-99.

65. Chiquet, M., *Regulation of extracellular matrix gene expression by mechanical stress.* Matrix Biol, 1999. **18**(5): p. 417-26.

66. Jarvinen, T.A., et al., *Mechanical loading regulates the expression of tenascin-C in the myotendinous junction and tendon but does not*

induce de novo synthesis in the skeletal muscle. J Cell Sci, 2003. **116**(Pt 5): p. 857-66.

67. Johnson, E.C., et al., *Global changes in optic nerve head gene expression after exposure to elevated intraocular pressure in a rat glaucoma model.* Invest Ophthalmol Vis Sci, 2007. **48**(7): p. 3161-77.

68. Drenser, K.A., et al., *Elevated levels of cystatin C and tenascin-C in schisis cavities of patients with congenital X-linked retinoschisis.* Retina, 2007. **27**(8): p. 1086-9.

69. Davis, J.T., et al., *Muller cell expression of genes implicated in proliferative vitreoretinopathy is influenced by substrate elastic modulus.* Invest Ophthalmol Vis Sci, 2012. **53**(6): p. 3014-9.

70. Kevany, B.M. and K. Palczewski, *Phagocytosis of retinal rod and cone photoreceptors.* Physiology (Bethesda), 2010. **25**(1): p. 8-15.

71. Green, W.R., *Histopathology of age-related macular degeneration.* Mol Vis, 1999. **5**: p. 27.

72. Dunn, K.C., et al., *ARPE-19, a human retinal pigment epithelial cell line with differentiated properties.* Exp Eye Res, 1996. **62**(2): p. 155-69.

73. Boulton, M. and J. Marshall, *Effects of increasing numbers of phagocytic inclusions on human retinal pigment epithelial cells in culture: a model for aging.* Br J Ophthalmol, 1986. **70**(11): p. 808-15.

74. Recktenwald, D.J., *Introduction to flow cytometry: principles, fluorochromes, instrument set-up, calibration.* J Hematother, 1993. **2**(3): p. 387-94.

75. Rizzo, J.F., 3rd, *Update on retinal prosthetic research: the Boston Retinal Implant Project.* J Neuroophthalmol, 2011. **31**(2): p. 160-8.

76. Nirenberg, S. and C. Pandarinath, *Retinal prosthetic strategy with the capacity to restore normal vision.* Proc Natl Acad Sci U S A, 2012. **109**(37): p. 15012-7.

77. Fan, Y.W., et al., *Culture of neural cells on silicon wafers with nano-scale surface topograph.* J Neurosci Methods, 2002. **120**(1): p. 17-23.